Title
Integrated Maneuvering Control Design And Experiments: Phase I

Authors
Hedrick, J. K.
Varaiya, P.
Narendran, V. K.
et al.

Publication Date
1995

CALIFORNIA PATH PROGRAM
INSTITUTE OF TRANSPORTATION STUDIES
UNIVERSITY OF CALIFORNIA, BERKELEY

Integrated Maneuvering Control Design and Experiments: Phase I

J.K. Hedrick
Pravin Varaiya
V.K. Narendran
Sei-Bum Choi

California PATH Research Report
UCB-ITS-PRR-95-15

This work was performed as part of the California PATH Program of the University of California, in cooperation with the State of California Business, Transportation, and Housing Agency, Department of Transportation; and the United States Department of Transportation, Federal Highway Administration.

May 1995

ISSN 1055-1425

Integrated Maneuvering Control Design and Experiments: Phase 1

Submitted By

J.K. Hedrick (P.I.)
Pravin Varaiya (Co P.I.)
V.K. Narendran
Sei-Bum Choi

Unviersity of California, Berkeley
Spring 1994

Integrated Maneuvering Control Design and Experiments

V. K. Narendran
S. B. Choi

Abstract

This report has been divided into two main sections. The first section addresses the issues of vehicle control during transition maneuvers in Intelligent Vehicle Highway Systems. Transition maneuvers include automatic lane change of vehicles and merging and splitting of platoons of vehicles in the automated highway system. The second part of the report addresses the issues involved in implementation of the longitudinal control laws for vehicle control in Automated Highway Systems.

A complete vehicle model has been presented. Simplifications are made to the model for controller design. Extensive nonlinearities in the engine dynamics and the six degree-of-freedom vehicle model prompts the usage of nonlinear control techniques to address the problem of vehicle control. We have a two-input (throttle/brake and steering), two-ouput (longitudinal spacing between vehicles and lateral deviation of the vehicle from the center of the lane) system for control.

Input-output linearization for multiple-input multiple output (MIMO) systems involves successive differentiations of the outputs to obtain the control inputs. This method is applied to the control of vehicles involved in transition maneuvers in AHS.

Limits on allowable vehicle accelerations and jerks during maneuvers necessitates the design of desired vehicle trajectories. We have adopted an open loop trajectory design method. A desired trajectory design method is proposed which is used with the designed controller and ensures that vehicle acceleration and jerk are within allowable limits specified for the maneuver. The proposed method is further modified to limit the maximum relative velocity attaiued between vehicles to satisfy the no-collision requirements.

Field Tests were performed to examine the validity of the vehicle longitudinal control laws. Even though simulation analysis of the existing control laws shows excellent performance the control laws must be modified to achieve suitable vehicle response in actual field tests. This part of the report addresses the issues involved in modifying existing control laws.

Executive Summary

This report describes the work performed under the second phase of studies on Integrated Maeuvering Control - Design and Experiments. At the end of phase 1 we had developed vehicle models and control algorithms to address only the longitudinal aspects of transition maneuvers in Intelligent Vehicle Highway Systems.

In this phase of study the vehicle model was extended to obtain a complete characterization of the vehicle dynamics - longitudinal as well as lateral dynamics. The report describes the detailed vehicle model and the simplifications to the model to obtain a model suitable for design of vehicle control laws. A controller has been designed based on the simplified vehicle model.

Since transition maneuvers involve a relatively higher spacing change compared to simple vehicle platooning the control law must ensure that control action is sufficiently smooth. This is achieved by prexcribing desired longitudinal and lateral trajectories that the vehicle must follow. This report also addresses "open-loop" trajectory design. The designed trajectory can then be modified to obtain some robustness.

The latter part of the report addresses the issues of implementation of longitudinal control laws. Field tests were performed with modified control laws to achieve the desired vehicle performance.

Contents

List of Figures

Chapter 1

Introduction

The Automated Highway System is primarily aimed at reducing congestion on highways through closer packing of vehicles per unit mile of the highway. The system will also result in improved safety on the highway and an easier and more comfortable ride for the individual. The longitudinal and lateral control studies of automobiles on the highway thus far have established the theoretical and practical feasibility of the concept .

This report looks at one aspect of the vehicle control part of the Intelligent Vehicle Highway Systems (IVHS) program. The research in the area has thus far been devoted to either pure longitudinal or pure lateral control of vehicles and the development of sensors and actuators needed for validation of the control laws. Focus is increasingly on issues such as transition and emergency maneuvers and fault detection and tolerance control.

The transition maneuvers address the problems of platoon formation and splitting, lane changing, entry and exit of vehicles to and from the automated lanes. These maneuvers must go hand-in-hand with system level decision making to allow for smooth smooth transition maneuvers.

1.1 Platoon Maneuvers

This project is aimed at investigating the intermediate maneuvers in automated highway systems. This includes the control of vehicles involved in changing lanes, joining platoons and splitting from platoons. The control of vehicles during these maneuvers constitutes the platoon maneuver control problem in Automated Highway Systems.

1.1.1 Platoon Maneuver Scenarios

The different types of transition maneuvers in the Automated Highway System have been described in Hsu et. al. 1991. The authors have described the protocols for the various transition maneuvers. We present a general case for each of the maneu-

vers. The type of maneuver chosen as a benchmark for the evaluation of our control algorithms is presented later.

figure 1.1 shows the various types of lane change operations. Some of the factors that determine the type of lane change operation are the velocities of the maneuvering and platoon vehicles, the time and distance constraints, and the types of vehicles involved.

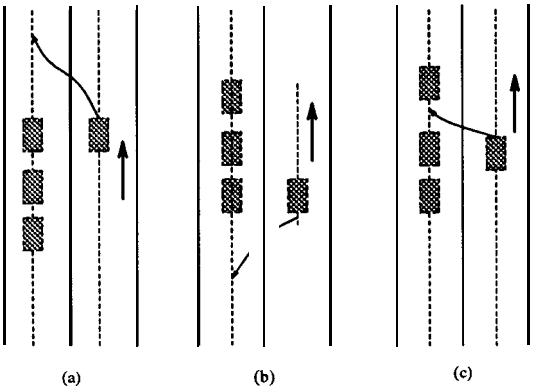

Figure 1.1: Types of Lane Change

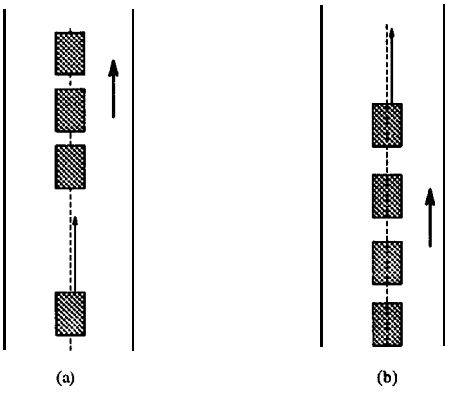

Figure 1.2: Merge and Split Procedures

Based on the longitudinal position and speed of the maneuvering vehicle relative to the position of the platoon on the highway, the vehicle can change its lane such that it joins the nearest platoon in the front of (type 3, figure 1.1(a)) or at the rear of the platoon (type 1, figure 1.1(b)). A lane change of type 1 is preferred over the mid-platoon lane change (type 2, figure 1.1(c)) from a safety point of view. Sometimes when the platoon size is big and we have a restriction on the maneuvering distance

for the maneuvering vehicle the mid-platoon lane change will be favored. In this case the vehicle changes lanes in such a manner that it enters the automated lane between two vehicles of the platoon. figure 1.2 shows the merging (1.2(a)) procedure wherein a vehicle in a particular lane joins either at the front(rear) of the platoon behind(ahead) it. The split procedure (figure 1.2(b)) involves vehicles that wish to leave a particular platoon. The merge and split procedures differ from the lane change procedure mainly in that the former involve vehicles all in the same lane of the highway which is not the case for the lane change operation in which a vehicle either enters or leaves the automated lane. In the former case the lane change operation will be followed by a merge maneuver to join the nearest platoon.

The automatic control of vehicles involved in such maneuvers is thus an important aspect of the Intelligent Vehicle Highway System Program. Chapter 2 addresses the various aspects of modeling and control of vehicles involved in such maneuvers.

The California Partners for Advanced Transit and Highway(PATH) have been developing automated vehicle control systems(AVCS) required for IVHS, and there are many engine control laws already developed and compared by simulation for longitudinal control of AVCS Choi 1993, Swaroop 1993.

However, in many cases, simulation results can be quite different from experimental results due to the effect of unknown modeling errors. In this report, several control laws are implemented on the test vehicles using a Quick-C compiler and XIGNAL a single tasking real-time scheduler developed at U.C. Berkeley. The performances of the control laws are compared by single vehicle speed tracking. The Polaroid ultrasonic ranging system is evaluated under several driving conditions. Two vehicle tracking control is performed using the ultrasonic sensor and radio transmitter/receivers.

Chapter 3 addresses the implementation and validation of control laws for vehicle following experiments. A vehicle model capturing the engine dynamics has been explained. The design of controllers for such a system has been outlined and the control laws have been tested on actual 1 vehicle and 2 vehicle experiments.

Chapter 2

Integrated Maneuvering Vehicle Control

The first step in designing controllers for vehicles involved in transition maneuvers is an identification of the various control tasks and subtasks for each type of maneuver. This is followed by a complete characterization of the vehicle dynamics. We are then in a position to design the control laws and make the necessary modifications to achieve the desired vehicle response in actual implementation of the control laws.

2.1 Maneuver Control Tasks

The process of the maneuver would require a higher, system level of control for making decisions regarding the type and time of initiation of the maneuver. The decisions could then be transmitted through communication links to the manevering vehicle and the vehicles of the platoon. The maneuver control task can be split into two parts.

1. Maneuver logic – The logic used to decide the order of maneuvering of the vehicles in the maneuver area. A maneuver logic is to be defined which will dictate the actual position and velocity of the maneuvering vehicle on the maneuver lane besides defining which vehicles from the platoon should be involved in the maneuver and in what order. Maneuver logic deals more with the method of assigning "which" vehicle will go "where" rather than "how" will it get there. Several algorithms have been proposed for the maneuver process but they deal with vehicles following the point or slot follower technique.

2. Vehicle control – control of the vehicles to accomplish the order desired. The design must take into the account the constraints imposed on the maneuver which include space considerations, vehicle capabilities, time constraints and above all passenger comfort and safety.

In the PATH program we have adopted a more decentralized or "asynchronous control" approach to the automated highway problem. Control of individual vehicles depends on the performance of the vehicles around it. This is in contrast to the centralized "synchronous" or "quasi-synchronous" approaches. A review of the existing literature in asynchronous control can be found in Narendran 1993.

2.2 Vehicle Model

Past studies of vehicle longitudinal control assume simple second and third order models of vehicles. Vehicle longitudinal control requires knowledge of the dynamics between the throttle and the observable parameter – the velocity of the vehicle. Vehicle models used for study of vehicle lateral control often neglect engine dynamics and assume that the required torque can always be produced by the engine.

Keeping the above issues in mind, a combined vehicle model was developed from two separate vehicle models – a lateral model, Peng 1992. and a longitudinal model, McMahon 1991, Cho 1989. A complete set of data was not available for the vehicles used for experimentation in the PATH program and hence the vehicle model used in this thesis is a hybrid model – the steady state engine maps of a Ford 5.0 liter V-8, rear wheel drive (RWD), front wheel steered (FWS) vehicle have been used as the front end to a vehicle model developed for a Toyota Celica, 2.4 liter, in-line 4, FWD, FWS vehicle, Peng 1992.

2.3 Engine Dynamics

The characterization of the engine dynamics closely follows the development of engine models by Cho and Hedrick, Cho 1992 and McMahon and Hedrick, McMahon 1991. Similar such models were used by McMahon in the development of vehicle models for

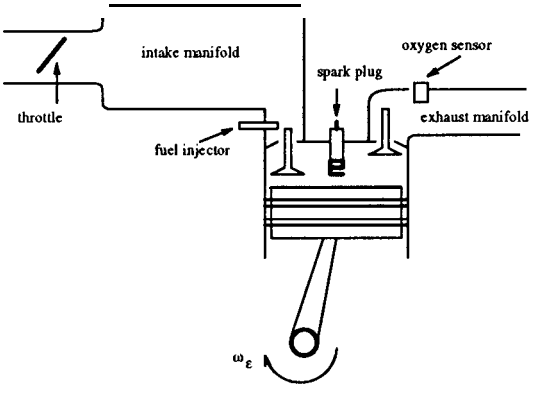

Figure 2.1: Engine schematic

longitudinal control in IVHS McMahon 1991. The earlier models were developed for 3.8 liter GM engines. The model that is presented here has been developed for a Ford vehicle – the Lincoln town car. A five state model was developed using the steady state maps. The model included two engine and three transmission states. This has been adapted for use along with the lateral part of the model.

The engine dynamics are captured through two engine states – mass of air in the intake manifold, m_a and engine speed, ω_e. Figure 2.1 is a schematic of the engine. The dynamics are represented as below:

$$\dot{m}_a = m_{ai} - m_{ao} \tag{2.1}$$

$$\dot{\omega}_e = (t_{net} - t_{pump})/j_e \tag{2.2}$$

where ,

$\dot{m}_{ai}, \dot{m}_{ao}$ are the mass rates of air flow into and out of the intake manifold respectively

$$\dot{m}_{ai} = \beta_1 PRI(p_m/p_a)TC(\alpha) \tag{2.3}$$

p_a, p_m are atmospheric and manifold pressures respectively , α is the throttle angle and PRI and TC are nonlinear functions.

t_{net}, t_{pump} are the net engine and pump torques respectively.

j_e is the effective engine inertia and β_1 is an engine constant.

Steady state engine maps were provided for the Lincoln Town car by the Ford Motor Company. These maps were used to develop table-look-up functions for $t_{net}, \dot{m}_{ao}$. The tables are indexed by two variables – ω_e and the pressure in the manifold, p_m both of which can be measured.

2.4 Drivetrain Dynamics

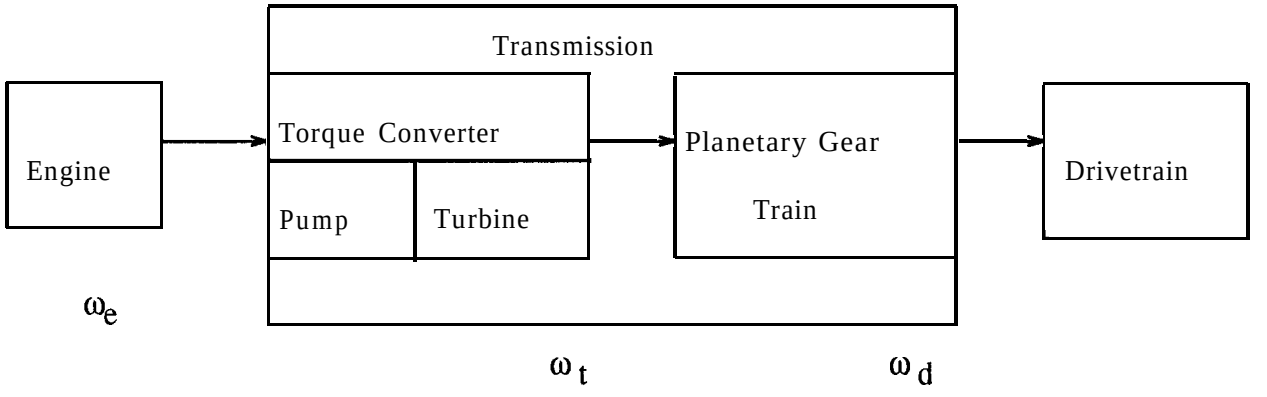

Figure 2.2: Transmission schematic

The model includes a torque converter and pump torque (engine side) and turbine torque (transmission side) are calculated from torque converter maps that are indexed

by the angular speed ratio across the torque converter. The gear shift dynamics have not been modeled. Figure 2.2 shows the transmission part of the vehicle. We have neglected shaft torque dynamics by assuming a rigid coupling between the turbine of the torque converter and the vehicle rear wheels.

The braking torque, t_{br} is represented in the form of a first order brake model given by:

$$\dot{t}_{br} = (t_{br,c} + t_{br})/\tau_b \tag{2.4}$$

where,
$t_{br,c}$ is the commanded brake torque.
τ_b is the time constant of the brake.
The brake input is the commanded brake torque.

2.5 Vehicle Sprung Mass Dynamics

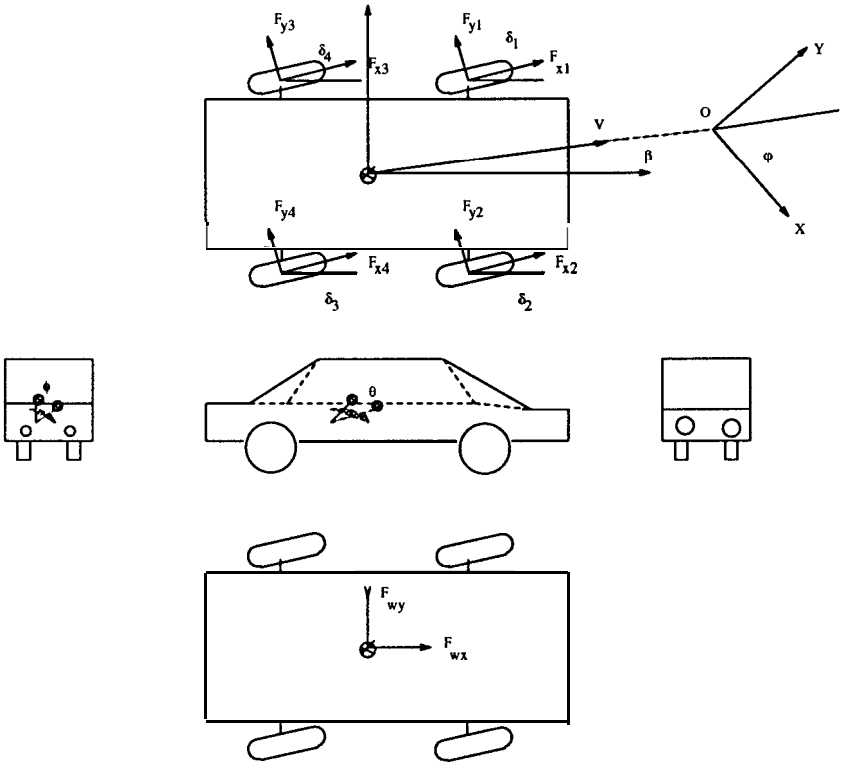

Figure 2.3: Vehicle Dimensions

The turbine torque forms the input to the 6-degree of freedom model that accounts for vehicle motion in the six directions of motion. The coupling between the

longitudinal and lateral part of the models comes through the tires and their effect is seen in the effect of the lateral tire force in the longitudinal direction.

The six degree of freedom model attempts to capture the dynamics of vehicle sprung mass in the six directions of motion i.e. longitudinal(z), lateral(y), vertical(z), roll($), pitch($\theta$) and yaw($). Figure 2.3 shows the angles and dimensions associated with the vehicle. Road superelevation and gradients have been neglected in the following vehicle equations. It is not apparent as to where the coupling in the two models comes from. The tractive forces appearing in the following equations also appear in the vehicle wheel equations. The driven wheels have the turbine torque as the input torque. These dynamics are represented in the equations listed below. A more detailed form of the following equations can be seen in Peng 1992.

$$
\begin{aligned}
m(\dot{V}_x - V_y\dot{\psi} + h_4\ddot{\theta} + h_2\dot{\phi}\dot{\psi} + h_2\phi\ddot{\psi}) &= \sum_{i=1}^{4} F_{A_i} - C_x V_x^2 - F_{roll} \\
m(\dot{V}_y + V_x\dot{\psi} - h_2\ddot{\phi} + h_4\dot{\theta}\dot{\psi} + h_4\theta\ddot{\psi}) &= \sum_{i=1}^{4} F_{B_i} - C_y V_y^2 \\
m(\dot{V}_z + V_x\dot{\chi}\beta - h_5\ddot{\theta}) &= \sum_{i=1}^{4} F_{P_i} - mg \\
I_x(\ddot{\phi} - \theta\ddot{\psi} - \dot{\theta}\dot{\psi}) - (I_y - I_z)\dot{\theta}\dot{\psi} &= M_x - \theta M_z \\
I_y(\ddot{\theta} + \phi\ddot{\psi} + \dot{\phi}\dot{\psi}) - (I_z - I_x)\dot{\phi}\dot{\psi} &= M_y + \phi M_z \\
I_z(\ddot{\psi} + \theta\ddot{\phi} - \ddot{\theta}\phi) - (I, - I_y)\dot{\phi}\dot{\theta} &= M_z + \theta M_x - \phi M_y
\end{aligned}
\tag{2.5}
$$

where,

XYZ	:	inertial frame of reference.
xyz	:	body fixed axis.
V_x, V_y, V_z	:	vehicle velocities in the x, y, z directions respectively.
$F_{A_i}(F_{B_i})$	:	longitudinal (lateral) force on the ith tire.
F_{P_i}	:	normal force on the ith tire.
F_{roll}	:	rolling resistance of tires.
C_x, C_y	:	vehicle drag coefficients in the x, y directions.
m	:	mass of the vehicle.
h_2, h_4, h_5	:	distances of the vehicle c.g. from the roll center, pitch center and ground respectiv
I_x, I_y, I_z	:	vehicle inertias about the x, y, z axis respectively.
M_x, M_y, M_z	:	vehicle moments about the x, y, z directions respectively.
β	:	vehicle side slip angle
χ	:	vehicle velocity angle $\chi = \psi + \beta$

vehicle slip angle (χ)is measured with respect to the sprung mass fixed co-ordinates while the vehicle yaw and velocity angles are measured with respect to the inertial coordinates.

The next few sections deal with the calculation of the tractive forces and moments appearing in the above equations.

2.5.1 Tire forces

The tire forces are calculated from a tire model developed by Peng Peng 1992. The tire model was developed using the Bakker-Pacjecka-Lidner model, Bakker 1989. This is a model that has been obtained through experimental study followed by nonlinear curve fit to obtain the longitudinal and lateral tire forces (f_{xi} and f_{yi}). Test data was obtained from a Yokohama P205/60R1487H steel belted radial tire. The tire forces for the ith wheel are given by the functional expressions:

$$\begin{aligned} f_{xi} &= f_{x0i}(\lambda_i, f_{zi}) \\ f_{yi} &= f_{y0i}(\gamma_i, f_{zi}) \end{aligned} \tag{2.6}$$

where,
λ_i, γ_i are respectively the slip ratio and slip angle of the ith tire.
f_{zi} is the normal force on the ith tire.
The slip ratio is defined as

$$\begin{aligned} \lambda_i &= \frac{r_{wi}\omega_{wi} - V_x}{r_{wi}\omega_{wi}} && \text{traction} \\ \lambda_i &= \frac{r_{wi}\omega_{wi} - V_x}{V_x} && \text{braking} \end{aligned} \tag{2.7}$$

ω_{wi} is the angular velocity of the ith wheel.
r_{wi} is the effective wheel radius of the ith tire.
The slip angle is the angle between the tire orientation plane and its velocity and is given by

$$\gamma_i = \delta_i - \zeta_i \tag{2.8}$$

where ζ_i is the angle between the forward speed of the ith tire and the vehicle body and δ_i is the ith wheel angle.

$$\begin{aligned} tan(\zeta_1) &= \frac{V_y + l_1\dot{\psi}}{V_x - \frac{s_{b1}\dot{\psi}}{2}} \\ tan(\zeta_2) &= \frac{V_y + l_1\dot{\psi}}{V_x + \frac{s_{b1}\dot{\psi}}{2}} \\ tan(\zeta_3) &= \frac{V_y - l_2\dot{\psi}}{V_x - \frac{s_{b2}\dot{\psi}}{2}} \\ tan(\zeta_4) &= \frac{V_y - l_2\dot{\psi}}{V_x + \frac{s_{b2}\dot{\psi}}{2}} \end{aligned} \tag{2.9}$$

The above equations allow us to calculate tire forces under pure traction or pure cornering maneuvers. Bakker, 1989, proposed a method to correct these forces under

the case of combined traction and cornering. For this we define normalized slip factors $\gamma^\star$ and $\lambda^\star$.

$$\lambda^\star = \frac{\lambda}{\lambda_{max}} \tag{2.10}$$

$$\gamma^\star = \frac{\gamma}{\gamma_{max}} \tag{2.11}$$

where, λ_{max} and γ_{max} are the values at which f_{xi} and f_{yi} achieve their peak values respectively. These are the f_{xi} and f_{yi} values from the traction only and cornering only tests. Now the correction factor is described as

$$\sigma^\star = [(\lambda^\star)^2 + (\gamma^\star)^2]^{.5} \tag{2.12}$$

Then the longitudinal and lateral tire forces are corrected by the following two equations.

$$f_{xi} = \frac{\lambda^\star}{\sigma^\star} f_{x0i}(\sigma^\star, f_{zi})$$

$$f_{yi} = \frac{\gamma^\star}{\sigma^\star} f_{y0i}(\sigma^\star, f_{zi}) \tag{2.13}$$

2.5.2 Suspension Forces

We have assumed a suspension system similar to what Peng, 1992, used for his lateral control study. The suspension consists of a spring and damper at each wheel. The deflections of the suspension joints can be calculated from geometry. The spring is assumed to be of the hardening type and is modeled as

$$F_{si} = C_{1i}(e_i + C_{2i}e_i^5) \tag{2.14}$$

where C_{1i}, C_{2i} are spring constants and e_i is the deflection of the suspension at the it h wheel.

The damper is a simple velocity type damper with the damper force F_{di} at the ith wheel being directly proprtional to the suspension deflection rate, $\dot{e}_i$.

The net suspension force is then given as the sum of the above two forces, calculated for each wheel.

2.5.3 Moments Acting on the Vehicles

The terminology used in this section has been defined in Table 1.1. The moments acting on the vehicle through the tires are computed from the following equations:

$$M_x = (\frac{s_{b1}}{2} + h_2\phi)F_{P_1} + (\frac{s_{b2}}{2} + h_2\phi)F_{P_3} - (\frac{s_{b1}}{2} - h_2\phi)F_{P_2} - (\frac{s_{b2}}{2} - h_2\phi)F_{P_4}$$
$$+(z - h_5\theta)\sum_{i=1}^{4} F_{B_i}$$

$$
\begin{aligned}
M_y &= (l_2 + h_4\theta)(F_{P_3} + F_{P_4}) - (l_1 - h_4\theta)(F_{P_1} + F_{P_2}) - (z - h_5\theta)\sum_{i=1}^{4} F_{A_i} \\
M_z &= (l_1 - h_4\theta)(F_{B_1} + F_{B_2}) - (l_2 + h_4\theta)(F_{B_3} + F_{B_4}) - (\frac{s_{b1}}{2} + h_2\phi)F_{A_1} \\
&\quad + (\frac{s_{b1}}{2} - h_2\phi)F_{A_2} - (\frac{s_{b2}}{2} + h_2\phi)F_{A_3} + (\frac{s_{b2}}{2} - h_2\phi)F_{A_4}
\end{aligned}
\tag{2.15}
$$

where, s_{b1}, s_{b2} are the front and rear treadwidths respectively.

These are the expressions of the moments in the unsprung mass axes and since the sprung mass rotates relative to the unsprung mass we need to multiply the above moments with a transformation matrix which finally gives us the right had side (RHS) of equations .

2.5.4 Wheel Equations

The angular velocities of the wheels (ω_{wi}) and the lateral displacement of the vehicle from the center of the lane (y_l) are also treated as state variables. The wheel equations are given by

$$
\begin{aligned}
j_{\omega_i}\dot{\omega}_{wi} &= \frac{T_{turb} * R_{\star}}{2} - \frac{t_{br}}{2} - r_{wi}F_{xi} \qquad \text{Vi} = 3,4 \text{ rear wheels} \\
j_{\omega_i}\dot{\omega}_{wi} &= -\frac{t_{br}}{2} - r_{wi}F_{xi} \qquad \text{Vi} = 1,2 \text{ front wheels}
\end{aligned}
\tag{2.16}
$$

The inputs to the model are the throttle angle, α, steering angle, δ_i (of the ith wheel), and the commanded brake torque, $t_{br,c}$. The net torque is a function of the throttle angle and engine speed. The steering angle δ_i appears implicitly in the tire forces.

In addition to these states we also keep track of the deviation of the vehicle c.g. from the center of the lane, y_r. y_r is obtained from the following equation:

$$
\dot{y}_r = V_y + V_x(\dot{\psi} - \dot{\psi}_d) \tag{2.17}
$$

2.6 Simplifications to Model For Control Purposes

The model is very nonlinear. t_{net} and $\dot{m}_{ao}$ are nonlinear functions of ω_e and p_m. In addition to this, the dynamics of the vehicle as captured by the six degree of freedom (6 d.o.f) model is also nonlinear. Some approaches, Peng 1992, linearize the system about various operating velocities and then apply linear control techniques. Unlike lane keeping where velocity changes are small, lane change maneuvers involve a wide range of velocity and acceleration changes and we hence have taken a nonlinear control approach to this problem.

Several assumptions were made to simplify the model for controller design purposes.

1. In the above equations we have neglected z-axis (suspension) and pitch dynamics.

2. No-slip assumption – we assume that there is no slip between the wheels and the road. This allows us to relate the vehicle speed to the engine speed.

$$V_x = R^* h \omega_e \tag{2.18}$$

where, R^* is the transmission ratio
h is the effective wheel radius.

3. Since platooning operations are essentially high speed and high gear operation of the vehicle, we assume that there is no slip across the torque converter. This allows us to use the following simplification to the engine dynamics:

$$\omega_e = (t_{net} - t_{load})/j_e \tag{2.19}$$

where t_{load} is given by
$t_{load} = R^*(h f_{tr} + t_{br})$
Hence this in effect allows us to reflect the vehicle load to the engine side and thus collapse the V_x and ω_e equations into one single equation.

4. For vehicle position control applications the intake manifold dynamics are sufficiently faster, Tomizuka 1993, than engine dynamics. Hence we can write:

$$m_{ai} \approx m_{ao} \tag{2.20}$$

$$m_{ao} \approx \beta_1 PRI(p_m/p_a)TC(\alpha) \tag{2.21}$$

In view of the above equations we can simplify the net torque calculation to obtain t_{net} as a function of ω_e and α.

5. The lateral tractive force is proportional to the vehicle slip angle and is given by:

$$F_{yi} = C_{si} s a_i \tag{2.22}$$

where, F_{yi} is the lateral force generated by the ith wheel.
C_{si} is the cornering stiffness of the ith wheel.

6. We have modeled a FWD, FWS vehicle and assume that $\delta_1 = \delta_2 = \delta_f$
$\delta_3 = \delta_4 = \delta_r = 0.0$

In view of the above assumptions the vehicle equations are as follows.

$$j_{eff}\dot{\omega}_e = r_1 r_{eff} + f_{wx} + r_1 m V_y \dot{\psi} + t_{net} - R^* t_{br} + \frac{2C_{sf}}{\omega_e}(V_y + l_1\dot{\psi}) - 2C_{sf} r_1 \delta_f^2$$

$$\dot{V}_y = \left(\frac{f_{wy}}{m} + r_2 f_{wx}\psi - \frac{A_1 V_y}{r_1\omega_e} - \frac{A_2\dot{\psi}}{r_1\omega_e} + \frac{2C_{sf}}{m}\delta_f\right)$$

$$\ddot{\psi} = -\frac{A_3 V_y}{r_1\omega_e} - \frac{A_4\dot{\psi}}{r_1\omega_e} + \frac{2C_{sf} l_1 d_s}{I_z}\delta_f$$

$$t_{br} = (t_{br,c} - t_{br})/\tau_b$$

where, r_{eff} is the effective wheel radius

$r_1 = r_{eff} R^{\star}$

$r_2 = \frac{r_1}{j_{eff}}$

$j_{eff} = j_e + m r_1^2$

$A_1 = 2\frac{C_{sf}+C_{sr}}{m}$ $\quad A_2 = 2\frac{l_1 C_{sf} - l_2 C_{sr}}{m}$

$A_3 = 2\frac{l_1 C_{sf} - l_2 C_{sr}}{I_z}$ $\quad A_4 = 2\frac{l_1^2 C_{sf} + l_2^2 C_{sr}}{I_z}$

In the preceding sections we have developed a complete vehicle model that can be used for vehicle control study. The model was validated by studying the open loop performance of the model to throttle/brake and steering inputs. The original longitudinal and lateral models were used as a yardstick to estimate the performance of the complete vehicle model. Extensive simulations yielded comparable performance results.

2.7 Controller Development

This section deals with the design of controllers for vehicles involved in transition maneuvers in IVHS. Transition maneuvers involve relatively more control action in a short period of time compared to vehicles in platoons, maintaining a specified spacing.

Designed controllers, in addition to assuring system stability through all regimes of operation, must also ensure a smooth transition from maneuver to platoon mode.

Even after model simplifications for control, the model is still very nonlinear. The nonlinearities enter in the form of the nonlinear steady state engine maps and also in the 6-d.o.f. model. Some research in lateral control (Peng 1992) is based on linear control theory. This is possible by linearizing the system about vehicle velocity. Then gain scheduled controllers are designed for the various velocity set-points. In this thesis we apply nonlinear control techniques to address the problem. One reason for this is the extensive nonlinearity in the engine dynamics part of the problem. In addition, lateral control aimed at lane keeping assumes a minimal velocity variation that allows for system linearization about various vehicle velocities. Transition maneuvers on the other hand involve a wider range of vehicle velocity variation and we hence adopt nonlinear control techniques.

In the previous section simplifying assumptions were made for controller purposes and the system can then be represented as below:

$$
\begin{aligned}
\dot{w}_e &= \tilde{f}_1(X) + c_{11}(X) t_{net} + c_{13}(X)\delta_f + c_{14}(X)\delta_f^2 \\
\dot{V}_y &= \tilde{f}_2(X) + c_{23}(X)\delta_f \\
\ddot{\psi} &= \tilde{f}_3(X) + c_{33}(X)\delta_f \\
\dot{t}_{br} &= \tilde{f}_4(X) + c_{42}(X) t_{br,c} \\
\ddot{y}_r &= \tilde{f}_5(X) + c_{53}(X)\delta_f
\end{aligned}
\qquad (2.23)
$$

In the equations above we have separated the terms relating to the brake torque t_{br} from $\tilde{f}_i(x)$ to obtain a more simplified form that now does not include the brake

dynamics i.e. if we consider the system such that t_{br} and not t_{brc} is the brake input to the system. We deal with the problem of obtaining the t_{brc} the actual brake input in the section addressing the actuator dynamics. Hence the system is now in the form below:

$$\begin{aligned}\dot{\omega}_e &= f_1(X) + c_{11}(X)t_{net} + c_{12}(X)t_{br} + c_{13}(X)\delta_f + c_{14}(X)\delta_f^2 \\ \dot{V}_y &= f_2(X) + c_{23}(X)\delta_f \\ \ddot{\psi} &= f_3(X) + c_{33}(X)\delta_f \end{aligned} \quad \textbf{(2.24)}$$

The throttle angle appears implicitly and for controller design purposes we treat t_{net} as the input since, with knowledge of the engine speed, we can use look-up tables to determine the desired throttle position. So our inputs are $t_{net}(t_{br})$ and δ_f. Since we use either the throttle algorithm or brake algorithm at any given time we hence have a two-input two-output system.

The system then is compactly referred as below:

$$\dot{X} = f(X) + g_1(X)u_1 + g_2(X, u_2) \quad \textbf{(2.25)}$$

where, $u_2 = \delta_f$, and $u_1 = t_{net}$(or $t_{br,c}$). The subsequent analysis assumes $u_1 = t_{net}$ and we explain how we can calculate t_{br} when the brake algorithm is in effect. $f(X) = [f_1(X)\, f_2(x)\, f_3(X)\, f_4(X)\ \ f_5(X)]^T$, $f_i(X)$ are nonlinear functions of the state. $g_1(X) = [0\ c_{11}\ 0\ 0\ 00]^T$ and $g_2(X, u_2)$ consists of all the terms associated with δ_f in equations (5)-(9).

2.7.1 System Outputs and Relative Degree

We would like to control the vehicle both longitudinally and laterally. Hence we select our outputs as the longitudinal spacing between the lead and maneuver vehicle and the lateral deviation of the vehicle (at the location of the deviation sensor) from the center of the lane. We would like to track a desired output trajectory. We define our outputs as follows:

$$\begin{aligned} h_1(X) = y_1 &= x - x_\ell \\ h_2(X) &= y_2 = y_s \end{aligned} \quad \textbf{(2.26)}$$

where, $x - x_\ell$ is the longitudinal spacing between the lead and maneuver vehicles:

$$y_s = y_r + d_s(\psi - \psi_d) \quad \textbf{(2.27)}$$

y_s is the lateral deviation of the lateral displacement sensor from the center of the road, d_s is the position of the magnetometer(for measuring lateral deviation (Peng **1992)** with respect to the vehicle c.g. and ψ_d is the desired yaw angle as obtained from the road radius curvature. y_r can be obtained from the following dynamic equation:

$$\ddot{y}_r = V_y + V_x(\dot{\psi} - \dot{\psi}_d) + \dot{V}_x(\psi - \psi_d) \quad \textbf{(2.28)}$$

In lane following approaches we can define our outputs in this fashion since the actual distance measured by the radar, $R \approx x - x_\ell$. This is true for short intervehicular spacing platoon operation. However for lane change operations this is not so and it is the R which must be chosen as an output instead of longitudinal spacing. Use of sensors such as the Qualimatrix optical ranging sensor, Qualimatrix 1993, sonar give us not only a measurement of R but also a lateral offset which allows us to calculate the longitudinal spacing. Hence we continue to use the longitudinal spacing instead of R as the output. Differentiating the output twice gives us equations of the type below:

$$\begin{aligned} \ddot{y}_1 &= \tilde{p}_1(X) + a_1 t_{net} + a_1' t_{br} + a_2 \delta_f + a_3 \delta_f^2 \\ \ddot{y}_2 &= \tilde{p}_2(X) + b_1 t_{net} + b_1' t_{br} + b_2 \delta_f + b_3 \delta_f^2 \end{aligned} \tag{2.29}$$

In order to input output (I/O) linearize the system we must first cast the system in the standard form for multiple-input mulitiple-output (MIMO) system I/O linearization, Isidori 1989. Since we have a non - affine input in the steering angle we will have to resort to implicit nonlinear equation solving to calculate δ_f. We avoid this by using dynamic extension, Descusse 1985, to define an additional state

$$\dot{\delta}_f = v_2 \tag{2.30}$$

results in an ill-defined vector relative degree for the system. Condition 1 for existence of a vector relative degree is satisfied. But the decoupling matrix is singular as is shown below

$$A(X) = \begin{bmatrix} \star & 0 \\ \star & 0 \end{bmatrix}$$

This is due to the fact that when the outputs are differentiated we arrive at the net torque (brake torque) 1 step earlier than the steering angle.

This can be avoided by defining yet another state

$$\dot{\alpha} = v_1 \tag{2.31}$$

Now the system with these two additional states has a well defined relative degreee of $[3\,3]^T$. An I/O linearized approach will necessitate differentiating the outputs 3 times. Thus we will have to differentiate the steady state engine maps which we would like to avoid.

2.7.2 Decoupled Control

During pure lane following maneuvers with the throttle held constant during the entire time period, one can assume that vehicle velocity is constant. This allows one to design a lateral controller based on linearized dynamics. Similarly in longitudinal control of vehicles, contribution of lateral tire forces during curve negotiation can be neglected and the problem can be treated as if no steering were being used.

Decoupled control is the use of decoupled longitudinal and lateral controllers for lane following along all sections of the highway. Pure lateral control is used during lane change. In effect the controller assumes no throttle variation during the lane change process. Realistically despite the throttle being held constant the vehicle velocity will drop during lateral maneuvers.

If we consider the lane change process in a straight section of the highway, the system can essentially be split up into a longitudinal and a lateral part.

$$\ddot{y}_r \approx V_y + V_x(\dot{\psi} - \dot{\psi}_d) \tag{2.32}$$

The above assumption simplifies calculation of the controller since we now have

$$\begin{aligned} \ddot{y}_1 &= \tilde{p}_1(X) + a_1 t_{net} + a_1' t_{br} + a_2\delta_f + a_3\delta_f^2 \\ \ddot{y}_2 &= \tilde{p'}_2(X) + b'_2\delta_f \end{aligned} \tag{2.33}$$

where, $\tilde{p}_i(X)$ represents all the state dependent terms that are not associated with the input terms.

Assuming that we know the model perfectly we can selecct δ_f such that the above equation yields exponentially decaying error dynamics. This is in effect only when the lane change process is in effect. So we can select

$$\delta_f = -\tilde{p'}_2(x) + \ddot{y}_{2d} - c_1\dot{e}_2 - c_2 e_2 \tag{2.34}$$

where, $e = y_2 - y_{2d}$

For longitudinal positioning of the vehicles involved in lane change, we assume δ_f is zero and hence can calculate t_{net} or t_{br}

$$t_{net} = -\tilde{p}_1\,(\mathrm{x}) - a_1' t_{br} + \ddot{y}_{1d} - c_1\dot{e}_1 - c_2 e_1 \tag{2.35}$$

where, $e_1 = y_1 - y_{1d}$

The advantage of using a decoupled controller along with the assumption on the y_r dynamics is that we do not have to deal with the input nonlinearities such as solving for *Sf*. Instead we get a direct expression for the steering angle. One of the main disadvantages is the absence of longitudinal control during the actual lane change process with the throttle being held constant. Steering action will result in a reduction in the velocity with the reduction depending on the severity of the lateral maneuver and if the lane change process involves a vehicle moving into the middle of a platoon then sufficient clearance must be given for the entering vehicle. We hence investigate simultaneous throttle and steering control to address the above issues.

2.7.3 Coupled Controller Design

Design of simultaneous longitudinal and lateral controllers is expected to increase the efficiency and decrease the time for lane change operations. In this section we examine the design of coupled controllers.

At any given time we use either throttle (t_{net}) or brake control (t_{br}).

Remark 1: If we are using throttle control the terms associated with the brake torque are included with $\tilde{p}_i(x)$ to give $p_i(x)$ and similarly the t_{net} terms are included with $\tilde{p}_i$ for brake control.

For the subsequent analysis we are assuming that only throttle control is in effect. The analysis for braking control is similar but requires a small extension of the algorithm being used for control.

We try to solve for the control directly rather than resort to dynamic extension, Isidori 1989, to define a relative degree and then I/O linearize the system. We would like to select $t_{net,des}$, $\delta_{f,des}$ such that we obtain error dynamics of the form

$$\ddot{e}_i + c_{i1}\dot{e}_i + c_{i2}e_i = 0 \qquad (2.36)$$

where, $e_i = y_i - y_{i,des}$ for i $= 1, 2$

c_{ij} are chosen Hurwitz Vi, j = $1, 2$.

From equations (30) and (37) we require:

$$\begin{aligned} a_1 t_{net,des} + \hat{a_1} t_{br,des} + a_2\delta_{f,des} + a_3\delta^2_{f,des} &= t_1 \\ b_1 t_{net,des} + \hat{b_1} t_{br,des} + b_2\delta_{f,des} + b_3\delta^2_{f,des} &= t_2 \end{aligned} \qquad (2.37)$$

$t_i = -\tilde{p}_i(X) + \ddot{y}_{i,des} - c_{i,1}\dot{e}_i - c_{i,2}e_i$ Vi = $1, 2$

From remark 1, we calculate $t_{net,des}$ from the above equations for throttle control by replacing $\tilde{p}_i$(x) in the above equations by p;(X) Where p;(X) $= \tilde{p}_i(x) + \hat{a_1} t_{br}$

Substituting for $t_{net,des}$ from the first of the two equations into the second it is seen that the coefficient associated with the $\delta^2_{f,des}$ term vanishes i.e. $b_2 = \frac{b_1 a_3}{a_1}$, ($b_2 = \frac{b_1' a_3}{a_1'}$ when solving for t_{br}), This allows us to solve for $\delta_{f,des}$ directly i.e. not having to resort to solving a quadratic equation. This is possible because of the particular choice of our outputs. Once we obtain $t_{net,des}$ we can solve for the desired throttle angle α_{des} using a table look-up function from the engine maps indexed by $t_{net,des}$ and w,.

Note :In case of braking control we calculate for $t_{br,des}$ from equations 38 and from remark $1, p_i(x) = \tilde{p}_i(x) + a1 t_{net}$

2.7.4 Robustness Issues

The above approach relies heavily on exact cancellation of nonlinearities. A method must hence be devised to take into account unmodeled dynamics. Hence we use sliding surface control to introduce some robustness to the proposed method.

We define two sliding surfaces $-S_\alpha, S_\psi$

$$\begin{aligned} S_\alpha &= \dot{e}_\alpha + \lambda_{\alpha,1} e_\alpha + \lambda_{\alpha,2} \int e_\alpha dt \\ S_\psi &= \dot{e}_\psi + \lambda_{\psi,1} e_\psi + \lambda_{\psi,2} \int e_\psi dt \end{aligned} \qquad (2.38)$$

where, $e_\alpha = y_1 - y_{1,des}$

$e_\psi = y_2 - y_{2,des}$

The only difference in the sliding approach is to calculate $t_{net,des}, \delta_{f,des}$ such that the sliding condition, Slotine 1991, is satisfied.

$$\begin{aligned} \dot{S}_\alpha &= -k_\alpha S_\alpha \\ S_\psi &= -k_\psi S_\psi \end{aligned} \tag{2.39}$$

By requiring that the above be satisfied we can cast the equations into a form similar to equations (16)-(17) and solve it in a similar fashion.

The brake algorithm is activated whenever α_{des} falls below a certain threshold value.

2.8 Actuator Dynamics

In the preceding sections we did not assume any dynamics for the actuators. Referring to the relative degree calculations it can be seen that if we have actuator dynamics of the form below we will require another differentiation before we reach the control inputs $\alpha_c(t_{brc})$ and δ_{fc}

$$\begin{aligned} \tau_\alpha \dot{\alpha} &= \alpha_c - \alpha \\ \tau_{\delta_f} \dot{\delta}_f &= \delta_f - \delta_f \\ \tau_b \dot{t}_{br} &= t_{brc} - t_{br} \end{aligned} \tag{2.40}$$

This will necessitate differentiating the engine maps which we would like to avoid.

One way to deal with this is to define additional surfaces of the form

$$S_{\alpha 2} = \alpha - \alpha_{des} \tag{2.41}$$

Then the first surface for the throttle will be used to calculate a synthetic input α_{des}. The second surface is then designed so as to drive α to α_{des}. So now by requiring that we have $\dot{S}_{\alpha 2} = -k_2 S_{\alpha 2}$ we can drive α_{des} to α. This procedure can be repeated for the other inputs as well.

2.9 Desired Trajectory Generation

An important part of control of vehicles during transition maneuvers is trajectory design. Step changes in desired positions can lead to high control action and can result in control saturation. In addition, this will lead to poor ride quality and can endanger the safety of the individual.

To alleviate this, a smooth trajectory can be designed which allows for smooth acceleration and deceleration of the vehicle. The trajectory must be designed to keep the vehicle jerk and acceleration within acceptable limits to provide reasonable ride quality. Hence the trajectory must be determined in some optimal fashion to minimize time and/or other performance criteria like fuel consumption such that constraints on allowable vehicle accelerations and jerks are not violatecl.

Design of a trajectory for the pure lane change maneuver is relatively the easiest since it requires a lateral position change of a fixed distance which is the distance between the centers of adjoining lanes. The final reference for trajectory design (i.e. center of the target lane) is fixed.

The problem of designing a trajectory for a moving final reference such as the platoon in the merge is more difficult. The desired trajectory for the merging vehicle must depend on the motion of the platoon it is trying to merge with. If the platoon acceleration is constant or zero, a smooth trajectory not violating the given acceleration and jerk conditions can be designed. The control problem should include some feedback on platoon velocity and position. The crux of the problem is in designing a trajectory and a controller to take into account acceleration variations in the platoon.

Trajectory planning for robot motion has been an active area of research for a number of years. Trajectory planning for robots is aimed at generating desired trajectories for robots which will avoid hitting of obstacles in its path. Several researchers have worked in the area of obstacle avoidance and navigation. We are more concerned with trajectory planning in an obstacle free environment and hence only cite the relevant references.

The most common trajectory design is one that minimizes the time of motion of the robot. Bobrow et.al., 1985, addressed this problem and more recently the work of Shiller 1989, Shiller 1992, and Shiller and Tarkiainen, Shiller 1993 address the design of time optimal trajectory paths. In Shiller 1992 the authors show that if the path is assumed, the time optimal motion is extremal in the acceleration. If jerk constraints are considered, a trajectory that is bang-bang in the jerk is achieved, Shiller 1993. The authors also present a computation algorithm for computing the time optimal tajectory. The main drawback in this method is prior knowledge of the path to be traversecl.

Designing trajectories to take into account input actuator torque bounds adds another dimension of complexity. Most trajectories are open-loop in the sense that they do not account for model uncertainties. So assumed allowable bound for input torques must be reduced to account for closed loop control action, Asada 1986. Some people have looked at closed loop optimal schemes Slotine 1985.

Trajectory design for robots is often a point to point start to stop motion. Hence a number of robot problems are of the fixed final reference type. The transition maneuver problem has an added complexity in the form of a moving final reference system.

This section mainly addresses the design of trajectories for moving final references – with or without acceleration. The case of lane change and merge of vehicles in absence of accelerations will then be a particular case of the generalized desired trajectory design.

In the previous section we designed controllers for the vehicle model chosen. The objective of the controller was to track the desired outputs as closely as possible. Since the steering and throttle/brake inputs are directly proportional to the desired trajectory, it is expected that the magnitude of control action will to some extent

depend on the magnitude of the desired acceleration.

We examine two ways of limiting the control action:

- Design of trajectories that take into account the closed loop control action.
- Design of open loop trajectories - does not take into account model uncertainties.

In this project we follow the open loop trajectory design. Hence the treatment of trajectory design is focussed more in this area. We do set up the problem for closed loop control action and mention some of the difficulties in solving this problem.

We design the trajectory for a general merge scenario. The platoon is represented by the last(first) vehicle of the platoon and is called the lead vehicle for purposes of this study and we are required to design a desired position trajectory of the merge vehicle which is joining at the back (front) of the platoon.

2.9.1 Terminology

In this section we define the parameters used for trajectory design in the subsequent sections.

$a_m(t), a_\ell(t)$	merge and lead vehicle accelerations at time t
$v_m(t), v_\ell(t)$	merge and lead vehicle velocities at time t
$sp(t)$	actual spacing at time t
$sp_d(t)$	desired spacing at time t
$sp_{d,tot}$	total desired spacing change $(sp_d(t_f) - sp_d(t_0))$
$vp(t)$	actual relative velocity at time t
$vp_{d,tot}$	total desired relative velocity change
$a_{m,max}, a_{\ell,max}$	merge and lead vehicle maximum accelerations
$j_{m,max}$	maximum jerk of merge vehicle
a_d	maximum allowable design acceleration $(a_d < a_{m,max})$
a_0	designed trajectory acceleration $(a_0 < a_d)$
t_c	climb time $(t_c = a_0/j_{m,max})$ of desired trajectory
t_m	maximum acceleration (decelaration) period of desired trajectory
t_h	zero acceleration (decelaration) of desired trajectory
t_0, t_f	initial and final times of merge maneuver

The objective of trajectory design is to design a time varying vehicle spacing trajectory with the knowledge of the following parameters:

1. $sp(t_0) = sp_d(t_0)$ - initital desired spacing is the iexisting spacing between the vehicles.
2. $sp_d(t_f)$- the final desired spacing – is usually the vehicle spacing for platoon operation.
3. $v_m(t_0) - v_\ell(t_0)$(must be same as $vp(t_0)$).

4. $v_m(t_f) - v_\ell(t_f)$(must be same as $vp(t_f)$). This should be zero since for continued platoon operation we should have constant intervehicular spacing

5. $a_m(t_0), a_\ell(t_0)$

6. $a_m(t_f)$(must be same as $a_\ell(t_f)$)

The initial spacing and relative vehicle velocity information is obtained from the radar while the acceleration of the lead vehicle is communicated to the following vehicle for feedback.

From the above information it is clear that to solve for the desired trajectory we have 3 pieces of information - the total spacing change, $sp_{t_f} - sp_{t_0}$, the total relative velocity change, $\dot{sp}(t_f) - \dot{sp}(t_0)$ and the total relative acceleration change, $\ddot{sp}(t_f) - \ddot{sp}(t_0)$. In addition we have constraints on allowable accelerations and jerks of the lead and merge vehicles respectively.

2.10 Closed Loop Trajectory design

In this section we examine the feasibility of posing the problem as an optimal control problem. Since we are addressing only the merge problem we can treat the system as a single-input single-output (SISO) nonlinear system with the output of concern being the longitudinal spacing between the lead and merge vehicles. Given a vehicle model for the merge vehicle of the form:

$$\begin{aligned} \dot{x} &= f(x,u) \\ y &= h(x) \end{aligned} \qquad (2.42)$$

where, $x \in \mathcal{R}^n$

$y, u \in \mathcal{R}$

$h(x) = x_m - x_\ell$

We would like to find a controller such that the control transfers the system such that the output is tranferred from $y(t_0)$ to some $y(t_f)$ without violating the system constraints.

This problem can be restated as an optimal control problem wherein we determine u based on the following criterion.

$$\min_{u \in U \subset \mathcal{R}} J = \int_{t_0}^{t_f} f'(x, u)dt$$

subject to constraints

$$\begin{aligned} \|a_m(t)\|_\infty &\leq a_{m,max} \\ \|j_m(t)\|_\infty &\leq j_{m,max} \end{aligned}$$

where J is the performance index and $f'(x,u)$ is a function that represents the function that we want to minimize - could be fuel consumption or time.

Problems with acceleration constraints are difficult to solve for systems of slightly higher order. In this case we have the additional problem of keeping the jerk within acceptable limits. A solution to is very difficult to find and we are still limited by the real time considerations of obtaining a solution in an actual vehicle involved in such maneuvers. In addition, the controller performs in the face of unmodeled dynamics in the system as well as a disturbance appearing in the form of the lead vehicle acceleration.

2.11 Open Loop Trajectory Design

From a practical and feasible point of view, open loop trajectory design seems to be a viable alternative. Looking at the problem from an actual driver's view, a typical driver would estimate the distance to the vehicle in front of him. If this is a vehicle of a platoon that he wishes to merge into, he uses this estimate to roughly accelerate (decelerate) and then decelerate (accelerate). The eye estimation provides a feedback for the driver. Hence this could be a method that could be applied. In the next few sections we define the various open loop trajectories that can be considered.

2.11.1 Polynomial Fits

Consider the situation where the desired spacing and desired relative velocity at t_0 and t_f is known. Hence we have 4 known values $-sp_d(t_0), \dot{sp}_d(t_0), sp_d(t_f), \dot{sp}_d(t_f)$. We can consider a desired spacing profile of the form

$$sp_d(t) = c_0 + c_1 t + c_2 t^2 + c_3 t^3$$

Now we can calculate $\dot{sp}_d$ and $\ddot{sp}_d$ from the above equation and we can use the four known values above to solve for the 4 coefficients c_0, c_1, c_2 and c_3. This method requires knowledge of t_f. Hence given a t_f, we can calculate this polynomial form to obtain a desired spacing.

2.11.2 Bang-Bang trajectory design

From a time optimal point of view, the minimum time trajectory is one whose acceleration profile consists of two regimes. A maximum acceleration phase followed by a minimum acceleration phase. The vehicle is assumed to have infinite jerk. This is shown in figure 2.4. This method has been shown here only to be used as a standard for comparison. The total spacing change is then given by:

$$sp_{d,tot} = a_d(t_m^2) \tag{2.43}$$

Due to jerk limitations the trajectory that is best suited for transition maneuvers is

one that is shown in figure 2.5. The desired relative acceleration profile can be given by the following equations.

$$\begin{aligned} a &= j_{max}(t - t_o) && t_o < t \leq t_1 \\ a &= a_d && t_1 < t \leq t_2 \\ a &= a_d - j_{max}(t - t_2) && t_2 < t \leq t_3 \\ a &= -a_d && t_3 < t \leq t_4 \\ a &= -a_d + j_{max}(t - t_4) && t_4 < t \leq t_5 \end{aligned} \tag{2.44}$$

where, $t_1 - t_0 = t_5 - t_4 = t_c = (\text{ad} - a_c)/j_{max}$

$a_,$ is the relative acceleration between the two vehicles at the start of the maneuver. The equations for calculating a_d are given in the next section. Consider the case where lead vehicle acceleration is zero and inital lead and merge vehicle velocity mismatch is zero. The only unknown in the above equation is t_m and is calculated from the required spacing change.

$$sp_{d,tot} = a_d(t_m^2 + 3t_m t_c + 2t_c^2) \tag{2.45}$$

We can use these equations to generate the desired relative velocity and desired spacing profiles by integration.

In the case where lead vehicle acceleration is zero and there is an intial velocity mismatch between the the two vehicles, $t_{m1} = t_2 - t_1 \neq t_4 - t_3 = t_{m2}$. The total area under the acceleration curve gives the net relative velocity change. However now we have two pieces of information – total change in spacing and total change in relative velocity. Thus we can use the above acceleration equations to solve for t_{m1} and t_{m2}.

2.11.3 Smooth Open Loop Trajectory Design

Instead of the bang-bang trajectory presented in the previous section we present a method of computing a smooth trajectory. Consider the desired relative acceleration trajectory shown in figure 2.6. The desired relative acceleration profile is given by:

$$\begin{aligned} a &= a_1(1 - cos(\omega(t - t_o)) && t_o < t \leq t_1 \\ a &= a_2(cos(\omega(t - t_1) - 1) && t_1 < t \leq t_2 \end{aligned}$$

In the above equations we assume that t_1 -to = $t_2 - t_1 = \frac{2\pi}{\omega}$ where w is the frequency. The above desired acceleration profile can be integrated to give the desired relative vehicle velocity and spacing profiles.

If the lead vehicle acceleration is zero throughout the maneuver and the initial relative velocity between the vehicles is zero then we have $a_1 = a_2 = a_0$, where a_0 can be calculated from:

$$a_0 = (sp_{d,tot}\omega^2)/(4 * \pi^2) \tag{2.46}$$

The frequency w is calculated to ensure that vehicle jerk is within allowable limits:

$$\omega = j_{m,max}/a_0 \tag{2.47}$$

In case $a_0 \geq a_d$ we can set $a_0 = a_d$ and introduce a no-acceleration period and the desired relative acceleration equations will be given by:

$$\begin{aligned} a &= a_d(1-cos(\omega(t-\text{ to})) && t_0 < t \leq t_1 \\ a &= 0 && t_1 < t \leq t_2 \\ a &= a_d(cos(\omega(t-t_2)-1) && t_2 < t \leq t_3 \end{aligned} \tag{2.48}$$

The total spacing change is used to calculate the time period for the zero acceleration phase.

If the lead vehicle acceleration is zero but there is an initial non zero relative velocity $a_1 \neq a_2$ and can be calculated by:

$$\begin{aligned} a_1 &= -\frac{1}{2}(vp(t_0)\frac{2\omega}{\pi} + \frac{\omega\, vp_{d,tot}}{2\pi}) \\ a_2 &= -\frac{1}{2}(vp(t_0)\frac{2\omega}{\pi} + \frac{3\omega\, vp_{d,tot}}{2\pi}) \end{aligned} \tag{2.49}$$

In the above two sections we did not consider the case of a lead vehicle acceleration. In the following section we suggest some modifications that can be made to the above trajectories to take into account lead vehicle acceleration.

2.12 Lead vehicle Acceleration

Hsu et. al, 1991 have worked on protocols for transition maneuvers in IVHS. A vehicle merges with a platoon ahead only when given a signal from the platoon ahead that it is not attempting any platoon maneuvers. This can be translated to an allowable acceleration limit of the platoon during the course of a merge. We can then use the upper bound of this acceleration to design the trajectory. This allows us to account for lead vehicle accelerations in the design of the desired trajectory.

In this method of using an open loop trajectory we assume that a controller has been designed to make y track y_d. We then assure non-violation of acceleration and jerk limits through proper design of the trajectory. We must therefore be able to use the form of the closed loop system to estimate the bounds required on the desired trajectories to ensure allowable merge vehicle performance.

2.13 Analysis for Desired Vehicle Accelerations

We assume that a controller has been designed for the system and we are assured of the following error dynamics:

$$\ddot{e} + c_1\dot{e} + c_2 e = 0 \tag{2.50}$$

where, $e = x_m - x_\ell - sp_d$

where, sp_d is the desired spacing

Substituting for $\ddot{e}$ in the above equation we have:

$$a_m = a_\ell + s\ddot{p}_d - c_1\dot{e} - c_2 e$$

$$|a_m| \leq |a_\ell| + |s\ddot{p}_d| - c_1|\dot{e}| - c_2|e|$$

From the above equation we can estimate the maximum merge vehicle acceleration given a lead vehicle acceleration. We calculate allowable desired trajectory acceleration from the following equations:

$$\begin{aligned} \ddot{a}_d &\leq min(a_{sp1}, a_{sp2}) \\ a_{sp1} &= |a_{m,max} - a_{\ell,pla}| - c_1|\dot{e}| - c_2|e| \\ a_{sp2} &= |d_{m,max} - d_\ell, pla| - c_1|\dot{e}| - c_2|e| \end{aligned} \tag{2.51}$$

where, $a_{\ell,pla}$ are the maximum platoon acceleration for merge.
$d_{m,max}, d_{\ell,pla}$ are the maximum decelerations of the merge vehicle and platoon respectively. We can quantize the magnitude of the remaining terms on the RHS of the above inequality to obtain a limit on the allowable desired relative acceleration of our trajectory.

The error dynamics however have been achieved through exact cancellation of the nonlinear terms. Hence we assume an error equation of the form below to estimate our error bounds and thus our desired relative acceleration maximum:

$$\ddot{e} + c_1\dot{e} + c_2 e = U_{max}$$

where, U_{max} represents an upper bound on the magnitude of unmodeled dynamics.

The error equation is linear and we can apply Laplace transform methods to obtain the following relation:

$$\hat{e}(s) = \frac{s\dot{e}(0)}{s^2 + c_1 s + c_2} + \frac{(1 + c_1)e(0)}{s^2 + c_1 s + c_2} + \frac{U_{max}}{s^2 + c_1 s + c_2}$$

In taking the Laplace inverse of the above equation we must consider two cases.

Real -ve roots:

$$\begin{aligned} e(t) &= (A_1 e^{-\beta_1 t} + A_2 e^{-\beta_2 t})\dot{e}(0) + (B_1 e^{-\beta_1 t} + B_2 e^{-\beta_2 t})e(0) \\ &\quad + (Q_1 e^{-\beta_1 t} + Q_2 e^{-\beta_2 t})U_{max} \end{aligned}$$

where, $A_1 = \frac{\beta_1}{\beta_1 - \beta_2}$ $\quad A_2 = \frac{\beta_2}{\beta_2 - \beta_1}$

$B_1 = \frac{1+c_1}{\beta_1 2 - \beta_1}$ $\quad B_2 = \frac{1+c_1}{\beta_1 - \beta_2}$

$Q_1 = \frac{1}{\beta_1 2 - \beta_1}$ $\quad Q2 = \frac{1}{\beta_1 - \beta_2}$

$\beta_1 = (c_1 + \sqrt{c_1^2 - 4c_2})/2$ $\quad \beta_2 = (c_2/\beta_1)$

Complex roots:

$$\begin{aligned} e(t) &= (e^{-\beta_1 t}cos\beta_2 t - \frac{\beta_1}{\beta_2}{}^{-\beta_1 t}sin\beta_2 t)\dot{e}(0) + \frac{1 + c_1}{\beta_2}e^{-\beta_1 t}sin\beta_2 t)e(0) \\ &\quad + \frac{U_{max}}{\beta_2}e^{-\beta_1 t}sin\beta_2 t) \end{aligned}$$

where, $\beta_1 = \frac{c_1}{2}$ $\beta_2 = \sqrt{4c_2 - c_1^2}/2$

From the above error equations we can calculate the corresponding derivatives to obtain expressions for $\dot{e}(t)$.

For real roots we have the following inequalities:

$$|e(t)| \leq (|A_1| + |A_2|)|\dot{e}(0)| + (|B_1| + |B_2|)|e(0)| + (|Q_1| + |Q_2|)|U_{max}|$$
$$|\dot{e}(t)| \leq (|A_1\beta_1| + |A_2|\beta_2)|\dot{e}(0)| + (|B_1\beta_1| + |B_2\beta_2|)|e(0)| + (|Q_1\beta_1| + |Q_2\beta_2|)|U_{max}|$$

For complex roots we have the following inequalities

$$|e(t)| \leq \sqrt{1 + \frac{\beta_1^2}{\beta_2^2}}|\dot{e}(0)| + |1 + \frac{c_1}{\beta_2}||e(0)| + |\frac{1}{\beta_2}||U_{max}|$$
$$|\dot{e}(t)| \leq (1 + \frac{|\beta_1|}{||\beta_2|})(\sqrt{\beta_1^2 + \beta_2^2}\dot{e}(0)| + |1 + c_1||e(0)| + |U_{max}|$$

From the above equations it is seen that the magnitude of errors and the derivative is dependent on the initial conditions and the unmodeled dynamics of the system. The initial error and error rate is a function of the accuracy of the radar sensor and can be made small by choice of a high precision radar system for range and range rate measurement. The merge vehicle acceleration is then upper bounded by the sum of the lead vehicle acceleration, desired relative acceleration, and the contribution of the unmodeled dynamics to vehicle acceleration. In short when designing a trajectory for the merge vehicle the lead vehicle accelerations and unmodeled dynamics play a role in determining how high the desired acceleration should be. This in turn will determine how fast the maneuver can be completed.

2.14 Safe Trajectory Design

Consider a vehicle trying to catch up with a platoon it wants to merge with. The trajectory will involve a gradual acceleration and a gradual deceleration phase. The trajectory must also be defined to take into account the case where the platoon goes into an emergency maneuver and the merging vehicle aborts the merging process. In such a case the merging vehicle must have sufficient distance to stop without a collision. Accounting for this scenario involves designing a trajectory which will limit the maximum relative velocity between the lead and merge vehicles.

For the following formulation we assume that the lead vehicle is travelling at constant velocity, v_1. It is assumed that initial velocity mismatch between the vehicles is zero. At time t_1 the lead vehicle goes into an emergency maneuver and starts decelerating at its maximum deceleration:

$$v_m(t) = \int_{t_0}^{t} a(\tau)d\tau + v_1 \tag{2.52}$$

$$sp_{cov}(t) = \int_{t_0}^{t}\int_{t_0}^{\hat{t}} a(\tau)d\tau d\hat{t} \tag{2.53}$$

$Sp_{cov}(t)$ is the reduction in spacing, as prescribed by the trajectory design, in time $t_1 - t_0$

Given a type of trajectory (i.e. Smooth or Bang-Bang) and a properly designed controller a desired relative acceleration profile *(a(t)* must be designed such that the following two conditions hold:

$$\int_{t_0}^{T} (v_m(\tau) - v_1) d\tau = Sp_{d,tot} \tag{2.54}$$

$$\frac{v^2(t_1)}{2a_{m,max}} - \frac{v_1^2(t_1)}{2a_{l,max}} \leq Sp_{d,tot} - Sp_{cov}(t_1) \tag{2.55}$$

The first condition ensures that the total desired spacing change is accomplished. The second one restricts the maximum relative velocity attained between vehicles for no collision in case of emergency deceleration. In the above equations, since we are considering a vehicle trying to catch up with a platoon the maximum accelerations referred above are negative. There are mainly two cases to consider and the second condition gets accordingly modified:

1. $a_{m,max} = a_{l,max}$

$$\frac{\Delta v^2(t_1)}{2a_{m,max}} + \frac{2v_1 \Delta v(t_1)}{2a_{m,max}} \leq Sp_{d,tot} - Sp_{cov}(t_1) \tag{2.56}$$

2. $a_{m,max} < a_{l,max}$

$$\frac{\Delta v^2(t_1)}{2a_{m,max}} + \frac{2v_1 \Delta v(t_1)}{2a_{m,max}} + \frac{v_1^2}{2}\left(\frac{1}{a_{m,max}} - \frac{1}{a_{l,max}}\right) \leq Sp_{d,tot} - Sp_{cov}(t_1) \tag{2.57}$$

This requirement can be imposed on any desired trajectory to determine the parameters of the trajectory.

The smooth trajectory that has been designed in the previous sections suffers from the disadvantage that the times of accleration and deceleration are fixed by the choice of the design acceleration. Then the time of acceleration is given by: $T_{acc} = 2\pi a_d / j_{m,max}$ Hence, a_d must lie between the two roots obtained from the following expression.

$$a_0 = a_2 \pm \sqrt{a_2^2 - \frac{4 j_{max} V_1}{\pi}} \tag{2.58}$$

In addition to this we have a condition on the allowable velocity at the start of the merge:

$$V_1 \leq a_2^2 \pi / 4 j_{max} \tag{2.59}$$

This is a very conservative estimate.

We examine the design of the "Feasible" bang-bang trajectory to take into account the no-collision requirement. Let $a_{m,max} = a_{l,max}$. In the following analysis we treat the no-collision requirement as an equality and can strengthen it by adding a safety distance to the right hand side. So we have two conditions to satisfy. Let us assume that the no-acceleration period is not required($t_h = 0$):

$$a_0(t_m^2 + 3t_m t_c + 2t_c^2) = sp_{d,tot} \tag{2.60}$$

$$\frac{\Delta v^2(t_1)}{2a_{m,max}} + \frac{2v_1\Delta v(t_1)}{2a_{m,max}} \leq Sp_{d,tot}/2 \tag{2.61}$$

where, $\Delta v(t_1) = a_0(t_m + t_c)$

$t_c = a_0/j_{m,max}$

We assume that the emergency maneuver starts at $t = T/2$ where $T = 4t_c + 2t_m$. We calculate t_m and a_0 from the above two equations.

If $a_0 \geq a_d$ we set $a_0 = a_d$ (hence fixing t_c as well. We introduce a no-acceleration zone (time $-t_h$) and the above equations are modified to give :

$$a_d(t_m^2 + 3t_m t_c + 2t_c^2 + (tm + t_c)t_h) = sp_{d,tot} \tag{2.62}$$

$$\frac{\Delta v^2(t_1)}{2a_{m,max}} + \frac{2v_1\Delta v(t_1)}{2a_{m,max}} \leq \frac{a_d}{2}(t_m + t_c)(t_m + 2t_c) \tag{2.63}$$

In this case we assume that the emergency maneuver occurs at $t = T - t_h = t_1$ where $T = 4t_c + 2t_m + t_h$. Since $a_0 = a_d$ is fixed, t_c is known. We calculate t_m and t_h from above.

In the case of differing maximum possible accelerations of the vehicles we get an extra term as presented earlier and the same procedure as above can be used to calculate the trajectory parameters. This method can also be extended to treat initial vehicle relative velocity and acceleration mismatches.

Table **1.1** shows the different trajectory parameters calculated for the "Feasible" bang-bang trajectory parameters. The following values were used for calculation :

$v_1 = 20m/sec$ $sp_{d,tot} = 50m$

$j_{m,max} = 10m/sec^3$ $a_{l,max} = -10m/sec^2$ For the case of $a_{m,max} < a_{l,max}$, $a_{m,max} = 8m/sec^2$

	$a_{l,max} = a_{m,max}$					$a_{l,max} > a_{m,max}$				
	a_0	t_m	t_h	Δv	T	a_0	t_m	t_h	Av	T
$t_h = 0$	2.1	5	-	10	10	.945	7.13	-	6.83	14.62
$t_h > 0$	2	3.98	1.61	8.35	10.36	.9	7.17	-	6.53	15.0

It must be noted that depending on initial conditions at the initiation of the merge the accelerations / decelerations may fall into the regime of emergency maneuvers. But the design has been worked out to be able to specify the maximum allowable acceleration and jerk limits. So in case the design does not allow for a safe, smooth maneuver – the maneuver can be aborted to go into emergency mode.

2.15 Proposed Trajectory Design

Analysis in the previous section allows us to calculate the design maximum acceleration of the desired profile. Now this value, in addition to the no-collision requirement can be used to generate a desired open loop trajectory of either the bang-bang type or the smooth type. We will be assured also that the vehicle acceleration and jerk will not violate the allowable limits. The algorithm is then:

1. Determine the design maximum desired relative acceleration using the analysis from the previous section
2. Determine total spacing and relative velocity change required
3. Use no-collision requirement and above information to calculated the parameters of the trajectory.

In the previous sections we have discussed the various ways to generate the desired spacing trajectory of the merging vehicle. The proposed design will ensure that the vehicle acceleration will not exceed allowable limits in closed loop operations.

2.16 Simulation Results

Despite being a non-minimum time trajectory, the smooth trajectory presented earlier has been used. The performance has been analyzed for the same transition maneuver scenario unless specified otherwise. The scenario involves two vehicles – a lead vehicle moving at 25 m/sec, 10 m ahead of the maneuver vehicle, also moving initially at 25 m/sec but in the adjoining lane. The lead vehicle represents the last car of a platoon behind which the maneuver vehicle wants to merge. The maneuver involves 3 phases – longitudinal positioning of the maneuver vehicle, a lane change and a longitudinal positioning to complete the merge. The results are with a model that neglects actuator delays. Both the steering and throttle actuator have rate saturation limits. The longitudinal and lateral spacing errors are with respect to the desired trajectory and are minimal. It can be seen in figure 2.8 and figure 2.10. that the maximum errors correspond to the periods of maximum control activity. The changes in the control are seen in figure 2.9 and figure 2.11 The variation of the "bird's eye view" or inertial position of the vehicles gives us an idea if the lane change occurs or not. Figure 2.7 shows the inertial position of the two vehicles.

The simulations indicate the effectiveness of the controller. Spacing errors are small and show how well the vehicle is able to follow the desired longitudinal and lateral spacing profiles. The smooth variations of the throttle and steering angles give us an idea of the corresponding longitudinal and lateral accelerations.

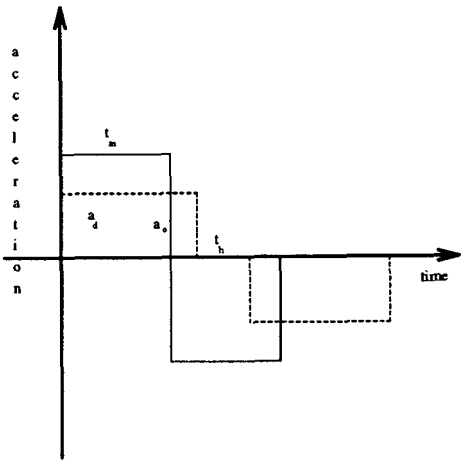

Figure 2.4: “Ideal” Minimum Time Trajectory

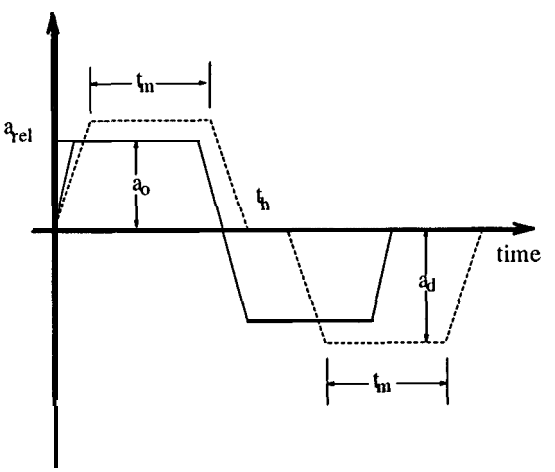

Figure 2.5: “Feasible” Minimum Time Trajectory

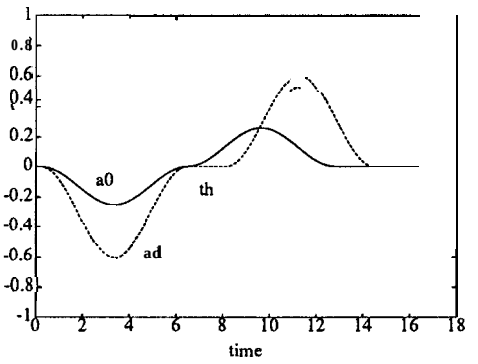

Figure 2.6: “Smooth” Trajectory

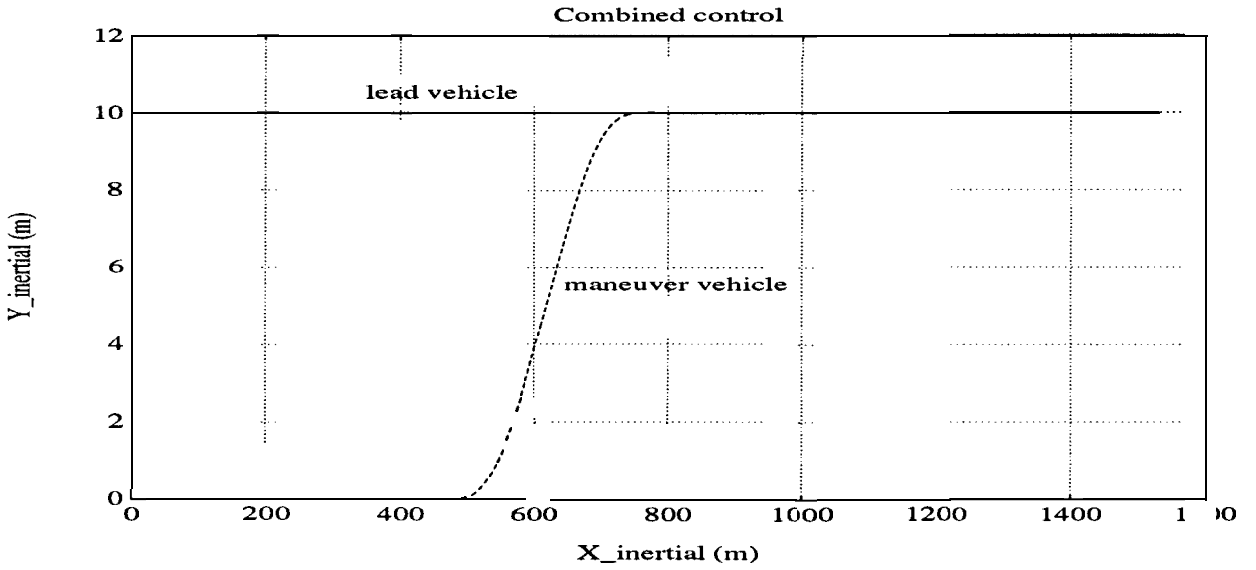

Figure 2.7: Inertial Position

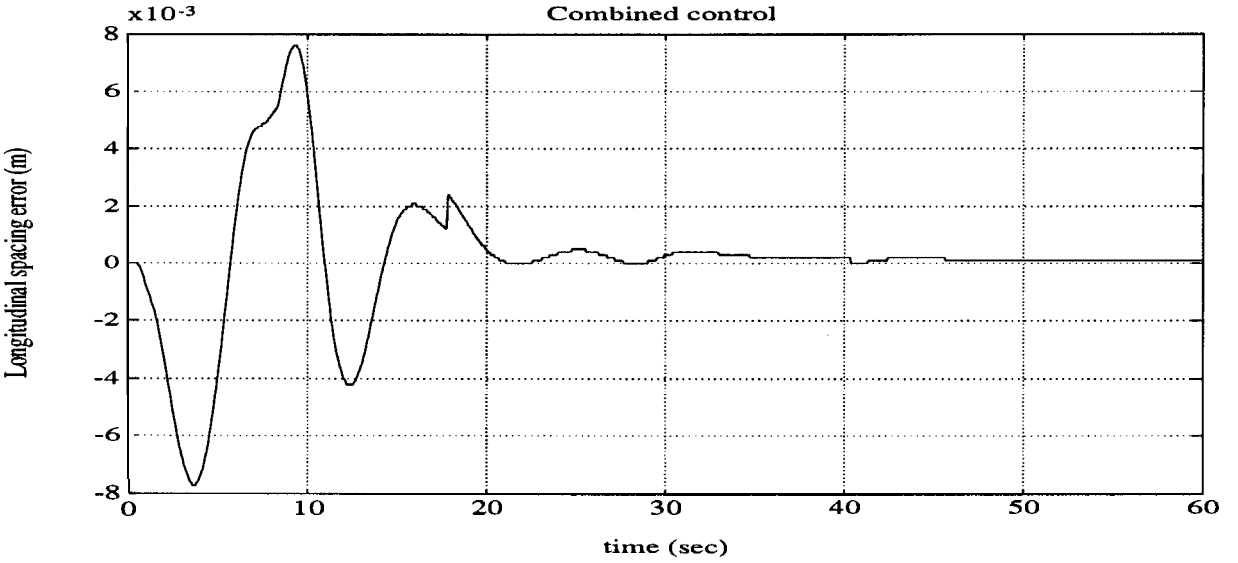

Figure 2.8: Longitudinal Spacing Error - Basic Controller

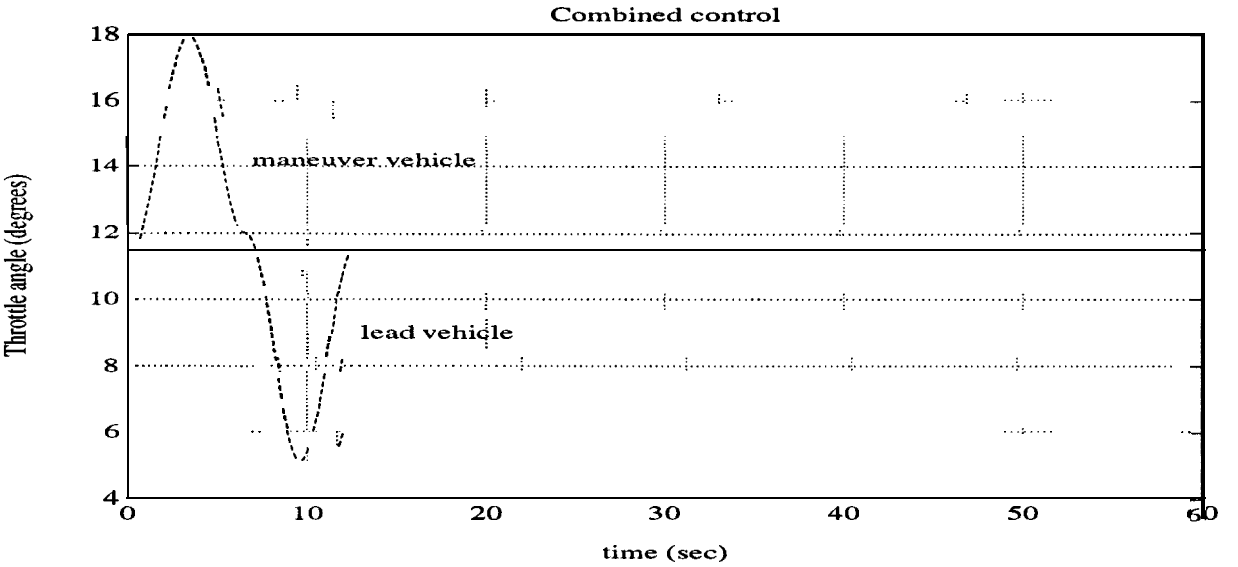

Figure 2.9: Throttle Angle - Basic Controller

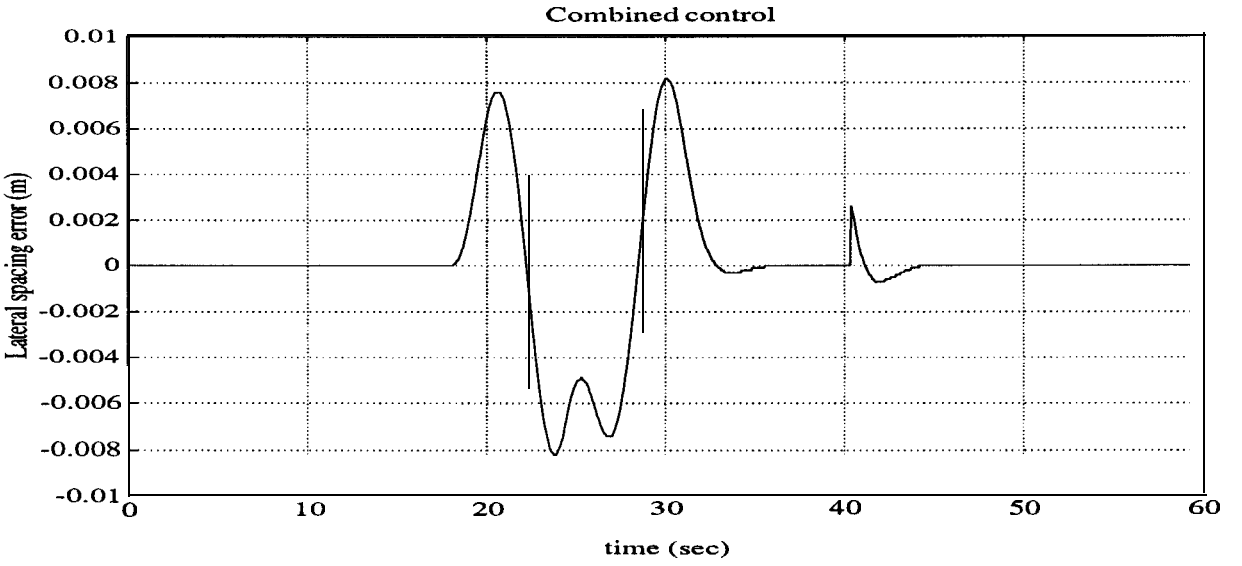

Figure 2.10: Lateral Spacing Error - Basic Controller

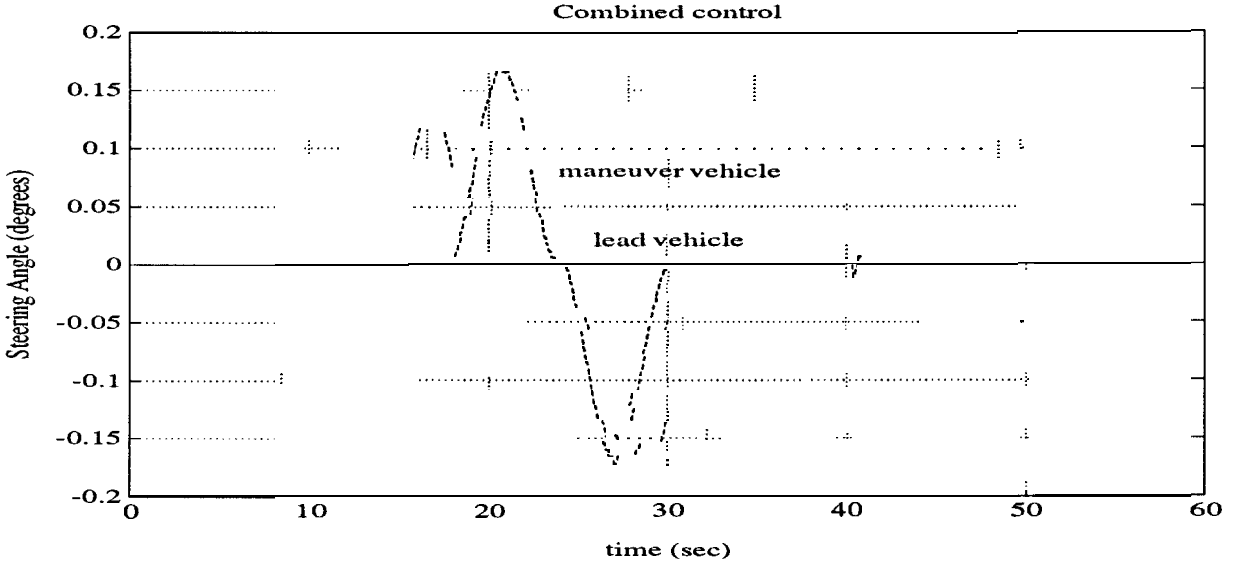

Figure 2.11: Steering Angle - Basic Controller

Chapter 3

Field Tests

In designing control laws for vehicles, simulation results can be quite different from experimental results due to the effect of unknown modeling errors. In this chapter, several control laws are implemented on the test vehicles using a Quick-C compiler and XIGNAL a single tasking real-time scheduler developed at U.C. Berkeley. The performances of the control laws are compared by single vehicle speed tracking. The Polaroid ultrasonic ranging system is evaluated under several driving conditions. Two vehicle tracking control is performed using the ultrasonic sensor and radio transmitter/receivers.

3.1 Vehicle Model for Longitudinal Control

This section gives a vehicle model for longitudinal speed control. The model is based on Cho and Hedrick's continuous engine model Cho **1989.** The sub-models considered are engine, intake manifold and torque converter.

3.1.1 Engine

The continuous engine model is described by Choi 1993:

$$\dot{\omega}_e = \frac{1}{I_e}\left[T_{net}(\omega_e, m_a) - T_L\right] \tag{3.1}$$

where T_{net} is the net combustion torque(indicated torque – friction torque), I_e the equivalent rotational inertia of the vehicle on the engine, ω_e the engine speed, m_a the mass of air in the intake manifold and T_L the external load on the engine. If each cylinder event is neglected and constant air-to-fuel ratio assumed, T_{net} is a function of only ω_e and m_a.

3.1.2 Intake Manifold

The assumptions in the modeling of the intake manifold are:

- the air in the intake manifold obeys the ideal gas law
- all properties(pressure and temperature) are uniform throughout the volume of the manifold
- the temperature of the air in the manifold is constant or changing very slowly
- the presence of fuel has no effect on the air flow
- the amount of exhaust gas recirculation (E.G.R.) is negligibly small

Neglecting the effects of individual intake strokes and pulsation of the air, the continuity equation of the manifold volume is:

$$\dot{m}_a = \dot{m}_{ai}(\alpha, P_m/P_{atm}) - \dot{m}_{ao}(\omega_e, m_a) \tag{3.2}$$

$$P_m V_m = m_a R T_m \tag{3.3}$$

where $\dot{m}_{ai}$ means the air flow rate through the throttle body, $\dot{m}_{ao}$ the air flow rate into the cylinder, α the throttle angle, P_m the manifold air pressure, P_{atm} the atmospheric air pressure, V_m the manifold volume, R the ideal gas constant and T_m the manifold air temperature.

3.1.3 Torque Converter

The torque converter consists of a pump attached to the engine and a turbine to the driving axle through a transmission. Neglecting the inertia of the transmission oil in the converter, it can be assumed to be a static element. On each side, the torque is related to the speed by:

$$T_t = \left(\frac{\omega_t}{C_{tr}}\right)^2 \tag{3.4}$$

$$T_p = \left(\frac{\omega_p}{C_{pr}}\right)^2 \tag{3.5}$$

where (T_t, ω_t, C_{tr}) and (T_p, ω_p, C_{pr}) mean the torques, the speeds and the capacity factors of the turbine and the pump. Since capacity factors are functions of the speed ratio($\triangleq \omega_t/\omega_p$), T_t, ω_t, T_p and ω_p are coupled each other, and the change of one affects the other three.

3.2 Control Laws

All the control laws in this section are derived under the assumption that the driving wheels have no-slip since the slip is not significant for the most of the normal operation conditions, i.e.:

$$V = R\,h\,\omega_e \tag{3.6}$$

where V means the vehicle speed, R the gear ratio from the engine to the wheels and h the tire radius of the driving wheels. If the platoon spacing error $S_1 (\triangleq P - P_{des}, \ \dot{P} = V)$ satisfies:

$$\ddot{S}_1 + 2\zeta\omega_n \dot{S}_1 + \omega_n^2 S_1 = 0 \tag{3.7}$$

where ζ and ω_n are design variables to be chosen depending upon the requirement of the control. Substituting equations **(3.1)** and (3.6) into equation (3.7), the desired engine torque for equation (3.7) to be satisfied is:

$$T_{net\text{-}des} = I_e \left[\dot{\omega}_{e\_des} - 2\zeta\omega_n (\omega_e - \omega_{e\_des}) - \frac{\omega_n^2 S_1}{R\ h}\right] + T_L \tag{3.8}$$

If the manifold air dynamics is neglected, $\dot{m}_{ai} = \dot{m}_{ao}$, and T_{net} becomes a function of ω_e and α, and the desired throttle angle α_{des} can be obtained as:

$$\alpha_{des} = \alpha_{des}(T_{net\_des}, \omega_e) \tag{3.9}$$

If the manifold air dynamics is not neglected, T_{net} is a function of ω_e and m,. Therefore, the desired air mass m_{a_des} for S_1 to satisfy equation (3.7) is obtained as:

$$m_{a\_des} = m_{a\_des}(T_{net\_des}, \omega_e) \tag{3.10}$$

Since m_{a_des} is not an explicit function of the control α, define:

$$S_2 \triangleq m_a - m_{a\_des} \tag{3.11}$$

and, if S_2 satisfies:

$$\dot{S}_2 = -\lambda_2 S_2, \ \lambda_2 > 0 \tag{3.12}$$

then, substituting equation (3.2) into equation (3.12):

$$\dot{m}_{ai\_des}(\alpha_{des}, P_m/P_{atm}) = \dot{m}_{ao} + \dot{m}_{a\_des} - \lambda_2 (m_a - m_{a\_des}) \tag{3.13}$$

or

$$\alpha_{des} = \alpha_{des}(\dot{m}_{ai\_des}, P_m/P_{atm}) \tag{3.14}$$

Here, $\dot{m}_{ao}$ is a function of ω_e and m_a, and using m_{a_des}(or P_{m_des}) instead of m_a(or P_m) makes the closed loop system more stable Choi 1993. Due to the same reason, P_{m_des} is used instead of P_m in α_{des}.

At the low(first and second) gear states, the engine is not connected to the driving wheels mechanically, and there exists torque converter slip. Therefore, at the very low wheel speed like starting from zero velocity, the slip is not negligibly small and the torque converter may need to be considered in the control, since the turbine torque is much bigger than the pump torque in that case and the control input becomes too much. During the normal to high wheel speed, the slip is negligible.

3.3 Single Vehicle Test

This section implements the control laws derived in section 3.3 on a test vehicle to follow the desired speed trajectories of an artificial lead vehicle. Since there exists no error in measuring the space and the rate of the change between the vehicles, the tracking performance can be much better than that in true vehicle following.

All the tests in this section were performed in first gear and there was no brake force on the wheels except that from the engine brake torque.

3.3.1 Simple Model

Figure 3.1 shows the test result of the control law given in equations (3.8) and (3.9) without the torque converter effect being compensated. Even though, critical damping(ζ = 1) is intended in the closed-loop, there exists a mode with zero or quite small damping, and the torque converter compensation is of no help in suppressing this mode(see figure 3.2). Figure 3.3 shows that the zero damping mode disappears at the higher vehicle speed or equivalently the higher engine speed. Due to this mode, the tracking performance deteriorates quickly as the frequency of the desired tracking speed profile is increased from 0.1 *Hz* to 0.2 *Hz*(see figures 3.2 and *3.4).*

3.3.2 Full Model

Figure 3.5 shows the test result of the control law given in equations (3.8),(3.10), (3.13) and (3.14) without the torque converter compensation. The transient error disappears quickly and the zero damping mode does not appear even after some maneuvering. At the very low vehicle speed, the turbine torque is much bigger than the pump torque and the control law which neglects this effect causes overshoot(see figure 3.5; 0 - 3 sec., 12 - 14 sec.). The throttle, and therefore the vehicle acceleration, can be smoothed without causing any delay by the compensation of the torque converter effect(see figure 3.6). This control law based on a full engine model does not have any bad effects like chattering at the higher vehicle(or engine) speed(see figure 3.7), and tracking the higher frequency speed profile is possible since the zero damping mode is suppressed (see figure 3.8).

3.3.3 Evaluation

The cause of the existence of the zero damping mode, at the low engine speed operation when the manifold dynamics is neglected, is studied for three possible cases after linearizing the system locally, Choi 1994

(i) Pure Input/Output Phase Lag

Neglecting the manifold air dynamics, equation (3.1) can be written as:

$$\begin{aligned}\omega_e &= \frac{1}{I_e}\left[T_{net}(\omega_e, \alpha) - T_L\right] \\ &\triangleq \frac{1}{I_e}\left[u - T_L\right]\end{aligned} \tag{3.15}$$

and the control law in equation (3.8) can be written as:

$$u \triangleq T_{net\_des} = I_e\left[\dot{\omega}_{e\_des} - 2\zeta\omega_n(\omega_e - \omega_{e\_des}) - \omega_n^2\int_0^t(\omega_e - \omega_{e\_des})\,dt\right] + T_L \tag{3.16}$$

Let u has first order lag with a time constant T due to the neglected manifold air dynamics, i.e.:

$$\dot{u}_1 = -\frac{1}{T}u_1 + \frac{1}{T}u \tag{3.17}$$

and

$$\dot{\omega}_e = \frac{1}{I_e}\left[u_1 - T_L\right] \tag{3.18}$$

Differentiating equation (3.17):

$$\ddot{u}_1 = -\frac{1}{T}\dot{u}_1 + \frac{I_e}{T}\left[\ddot{\omega}_{e\_des} - 2\zeta\omega_n(\dot{\omega}_e - \dot{\omega}_{e\_des}) - \omega_n^2(\omega_e - \omega_{e\_des})\right] + \frac{T_L}{T} \tag{3.19}$$

Let

$$\dot{\omega}_{e\_des} = \ddot{\omega}_{e\_des} = \dot{T}_L \triangleq 0 \tag{3.20}$$

$$u_1 = v_1 \tag{3.21}$$

$$\dot{u}_1 = v_2 \tag{3.22}$$

then, equations (3.18),(3.19), (3.21) and (3.22) give:

$$\begin{bmatrix}\dot{\omega}_e \\ \dot{v}_1 \\ \dot{v}_2\end{bmatrix} = \underbrace{\begin{bmatrix} & I_e & \\ 0 & 0 & 1 \\ \frac{\omega_n^2 I_e}{T} & -\frac{2\zeta\omega_n}{T} & -\frac{1}{T}\end{bmatrix}}_{\triangleq A}\begin{bmatrix}\omega_e \\ v_1 \\ v_2\end{bmatrix} + constant \tag{3.23}$$

The characteristic equation of a matrix A is:

$$\lambda^3 + \frac{1}{T}\lambda^2 + \frac{2\zeta\omega_n}{T}\lambda + \frac{\omega_n^2}{T} = 0 \tag{3.24}$$

When T, ζ and ω_n are 0.17, 1.0 and 2.5 as those in figure 2.1, the solutions of equation (3.24) are λ_1 = -1.64, $\lambda_{2,3}$ = -2.12 $\pm$ i 4.24, and the equivalent cycle time of $\lambda_{2,3}$ is 1.48 sec. This is very close to the cycle time in the test($\approx$ 1.7 sec). However, the damping of $\lambda_{2,3}$ is too big to have a zero-damping-like mode.

(ii) Pure Input/Output Time Delay

Now assume that the control input u has pure time delay t_d, i.e.:

$$\begin{aligned}\omega_e &= \frac{1}{J_e}\left[T_{net}\ (\omega_e,\ \alpha) - T_L\right] \\ &\triangleq \frac{1}{I_e}\left[u_1 - T_L\right]\end{aligned} \tag{3.25}$$

$$u = I_e\left[\dot{\omega}_{e\_des} - 2\zeta\omega_n\,(\omega_e - \omega_{e\_des}) - \omega_n^2\int_0^t(\omega_e - \omega_{e\_des})\,dt\right] + T_L \tag{3.26}$$

$$u_1(t) = u(t - t_d) \tag{3.27}$$

Let $\dot{\omega}_{ed} = \ddot{\omega}_{ed} = \dot{T}_L \triangleq 0$ again, then equations (3.25) - (3.27) give:

$$\text{k(t)}\ \cdot\text{i-}\ 2\zeta\omega_n\dot{\omega}_e(t - t_d) + \omega_n^2\,\omega_e(t - t_d) = 0 \tag{3.28}$$

Let

$$\omega_e(t) = e^{i\lambda t} \tag{3.29}$$

and substituting equation (3.29) into equation (3.28):

$$-\lambda^2 + i\,2\zeta\omega_n\,\lambda\,e^{-i\lambda t_d} + \omega_n^2\,e^{-i\lambda t_d} = 0 \tag{3.30}$$

If equation (3.30) gives a real valued solution (λ, t_d), then the closed-loop system may have a zero damping mode when the time delay is as much as t_d. Since the solution λ of equation (3.30) is given as:

$$\lambda = \sqrt{2\zeta^2 + \sqrt{4\zeta^4 + 1}}\,\omega_n \tag{3.31}$$

when ζ = 1 and w,, = 2.5, λ = 5.1 and equivalently the cycle time of the mode is 1.23 sec and the required time delay to have that mode is 0.26 sec. This time delay is too much to think of in this system. Therefore, the system can not have a zero damping mode due to the pure time delay alone.

(iii) Phase Lag Combined with Time Delay

Assume that the control input has both phase lag and time delay, i.e.:

$$\dot{\omega}_e = \frac{1}{I_e}\,[u_1 - T_L] \tag{3.32}$$

$$u = I_e \left[\dot{\omega}_{e\_des} - 2\zeta\,\omega_n(\omega_e - \omega_{e\_des}) - \omega_n^2 \int_0^t (\omega_e - \omega_{e\_des})\,dt\right] + T_L \tag{3.33}$$

$$\dot{u}_1 = -\frac{1}{T}\,u_1(t) + \frac{1}{T}\,u(t - t_d) \tag{3.34}$$

Let

$$\dot{\omega}_{e_des} = \ddot{\omega}_{e_des} = \dot{T}_L \triangleq 0 \tag{3.35}$$

then, equations (3.32) - (3.34) give:

$$\dddot{\omega}_e(t) + \frac{1}{T}\,\ddot{\omega}_e(t) + \frac{2\zeta\,\omega_n}{T}\,\dot{\omega}_e(t - t_d) + \frac{\omega_n^2}{T}\,\omega_e(t - t_d) = 0 \tag{3.36}$$

Let equation (3.36) have a zero damping mode, i.e. $\omega_e(t) = e^{i\lambda t}$, then equation (3.36) gives:

$$-\frac{1}{T}\,\lambda^2 + \frac{2\zeta\,\omega_n}{T}\,\lambda\,\sin\lambda t_d + \frac{\omega_n^2}{T}\,\cos\lambda t_d = 0 \tag{3.37}$$

$$-\lambda^3 + \frac{2\zeta\,\omega_n}{T}\,\lambda\,\cos\,\lambda t_d - \frac{\omega_n^2}{T}\sin\lambda t_d = 0 \tag{3.38}$$

If equations (3.37) and (3.38) have a real valued solution (λ, t_d), then the closed-loop system can have a zero damping mode. When T, ζ and ω_n are 0.17, 1.0 and 2.5 as those in figure 3.1, equations (3.37) and (3.38) give a solution λ = 4.2, i.e. the cycle time of the zero damping mode is 1.5 sec, and the time delay required to get this mode is t_d = 0.15 sec. The cycle time is very close to that in the test($\approx$ 1.7 sec) and the amount of the time delay is reasonable. The intake-to-torque production time delay is around 35 ms at 1500 rpm Cho 1989 and the throttle actuation time delay is around 40 ms. In addition, at the first and the second gear states, torque converter is observered to give 60 - 80 ms time delay. Therefore, the total input/output time delay is 135 - 155 ms, and this is the amount just enough to generate a low-frequency zero damping mode in the closed-loop system. The amount of time required to generate this mode by the pure time delay alone is 260 ms, and 110 ms safety margin is obtaiued by considering the manifold air dynamics in the control.

3.4 Ultrasonic ranging system

3.4.1 Introduction

This section describes Polaroid ultrasonic ranging system. This system uses 50 kHz ultrasouic sound and the operating range is approximately 0.15 - 10 meters. The typical absolute accuracy is ± 1 % of the reading over the entire range (see figure 3.10). In operation, a pulse is transmitted toward a target and the resulting echo is detected. The elapsed time between initial transmission and echo detection can then be converted to distance with respect to the sound of speed.

The speed of sound at 20°C is 343.2 m/s, and increases proportional to the square root of the ambieut air temperature. It varies only slightly with humidity(max 0.35 % at 20°C) and is virtually independent of pressure and, thus, of height above sea level - Polaroid Corporation.

3.4.2 System Description

The system should respond only to echoes from objects which are in a given solid angle around the transmit axis. Any echo signal from an object far off axis is undesirable. Transducer diameter and transmit frequencies were chosen so that an object at 25 cm distance at an angle of 20 degrees gives an echo about 20 dB weaker than the same object placed on axis at the same distance. If the object is moved from 25 cm to a distance of 5 m on axis, the echo will fall off by about 60 dB.

If a constant amplification were used the operating range would be severely limited. The situation is even worse since different objects at different temperatures and humidities will vary in echo strength by as much as 20 - 30 dB. Therefore, it is desirable to vary the amplification with distance: low amplification for near distance echoes, high amplification for far distance echoes. Since the roundtrip time for the signal is proportional to the distance, it means that the amplification should be increased as a function of time. The gain should not produce a constant signal level of a given object at different distances. It is assumed that nearer objects tend to be smaller and therefore relatively more gain is desirable (figure 3.9). Large amplified signals improve the accuracy of the distance determination, but make the system more sensitive to the small particles between the transducer and the target, Polaroid Corporation.

3.4.3 Field Test

The ultrasouic ranging system was tested on California Highway Patrol(CHP) Academy test track at Sacramento. It is a windy area and the track is dusty. The test was performed using two Lincoln TownCars; one following the other. Figure 3.10 shows that the system works well at the low vehicle speed and within its operating range. However, figure 3.11 shows that, even when the distance is within the operating

range, it gets only noise at the higher vehicle speed. There are three possible sources of the noise: wind noise, tire noise and dust/particles. The effect of the wind noise can be checked easily by driving the vehicle at the high speed without any target vehicle, and it was found not to be a source of the noise. Second, it was tested using two vehicles at the high speed but in a relatively clean section of the track, and there was not much noise. So, it is concluded that the noise comes from the cloud of dust kicked up by the lead vehicle at the appropriately high speed. The noise disappears if the vehicles drive at a very short distance for the kicked up dust to appear between the vehicles.

As described in section 3.4.2, the system gain is varied such that it is very sensitive to any particles which are very close to the transmitter. Another problem of the sonar system is that the transmitter can not be concealed. As a result, all the transmitters have been found to be damaged after driving the vehicles at 100 km/h for 10 hours. So, this system may not be appropriate to be used in a dusty environment.

3.5 Multi-Vehicle Test

In section 3.3, two longitudinal control laws were compared by field test, and the control law based on a full engine model including the manifold dynamics showed the best tracking performance.

In this section, multi-vehicle closed-loop control is tested using the best control law at low speed cruising. The control law gets the distance and the closing rate from the ultrasonic ranging unit and the lead vehicle speed transmitted by radio.

Figure 3.12 shows the test result of the multi-vehicle tracking control. The ranging unit works well most of the time since the vehicle speeds are very low, and the distance between the two vehicles converges to the preset value exponentially as desired. The throttle is not chattering much, so the ride quality, i.e. the vehicle acceleration and jerk, is quite smooth.

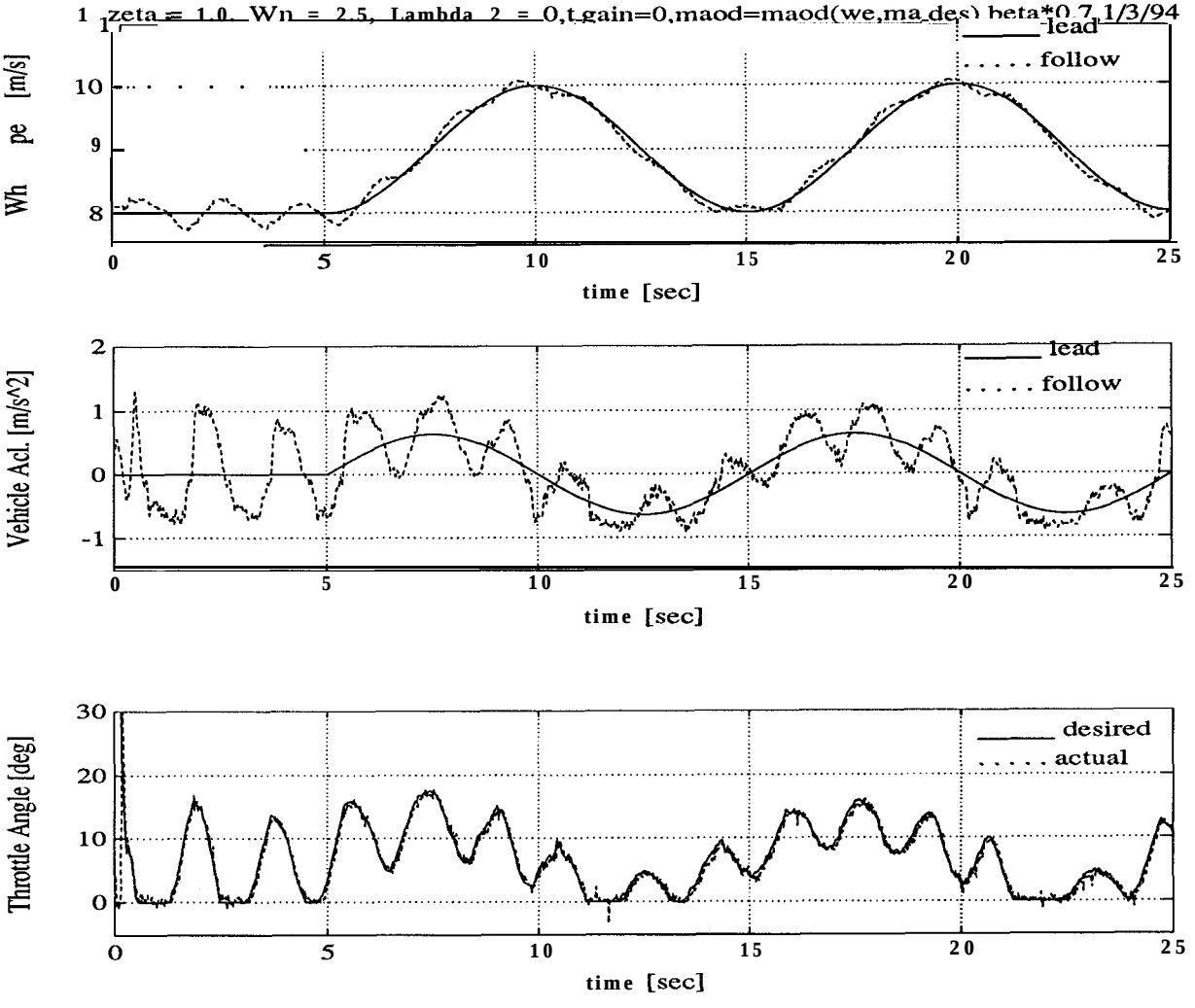

Figure 3.1: Single vehicle tracking control; simple model, no torque converter

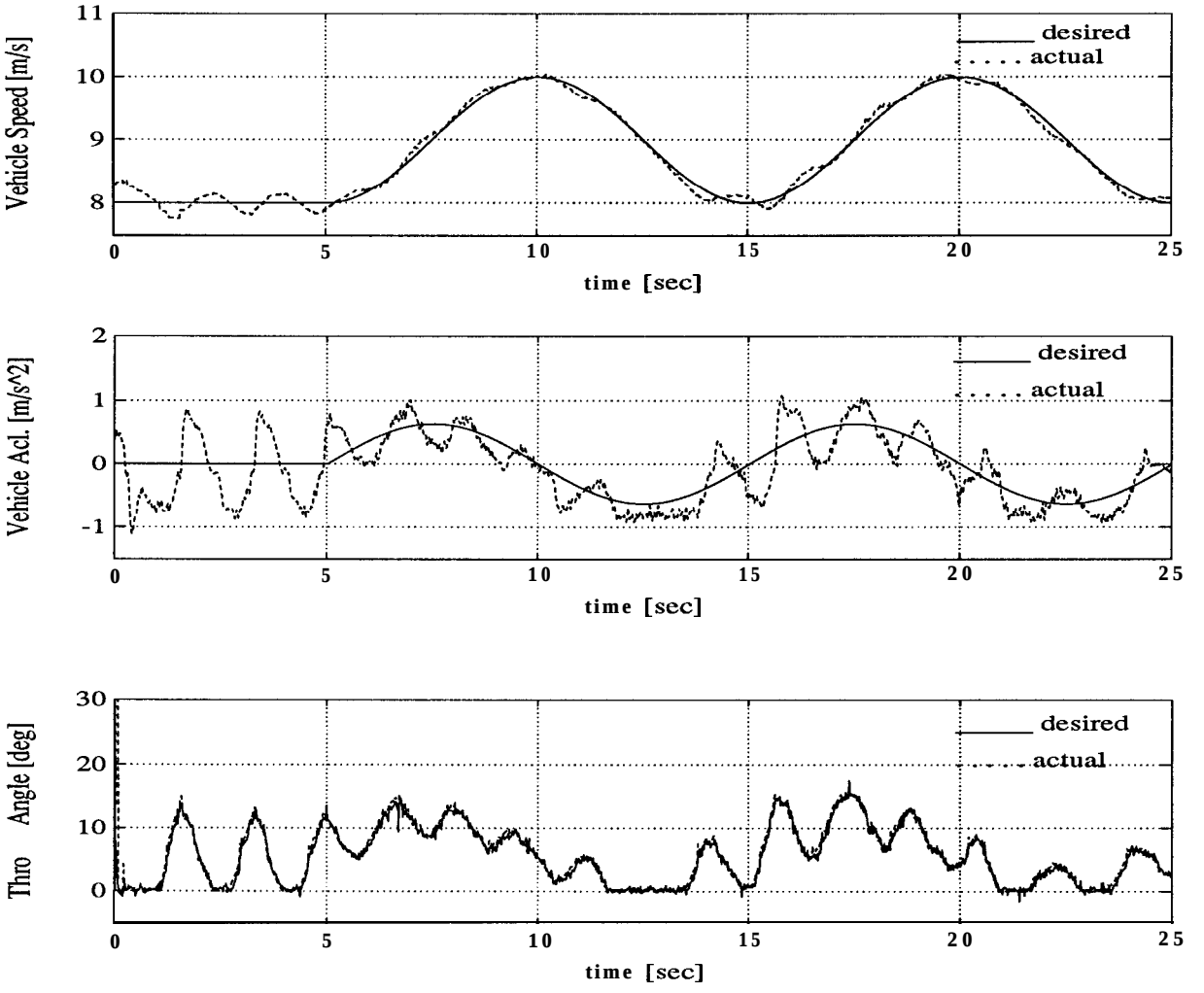

Figure 3.2: Single vehicle tracking control; simple model with torque converter

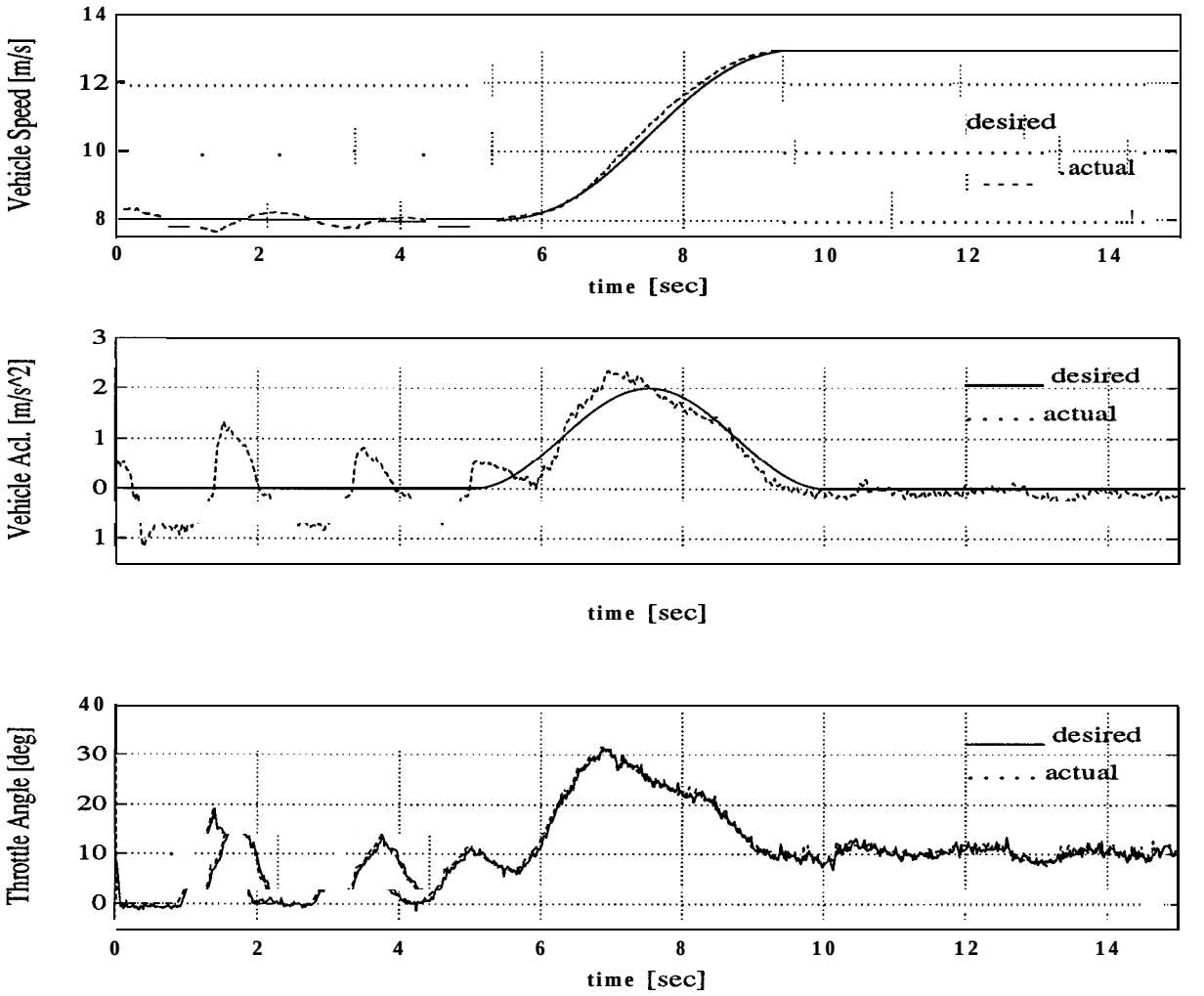

Figure 3.3: Single vehicle tracking control; simple model with torque converter

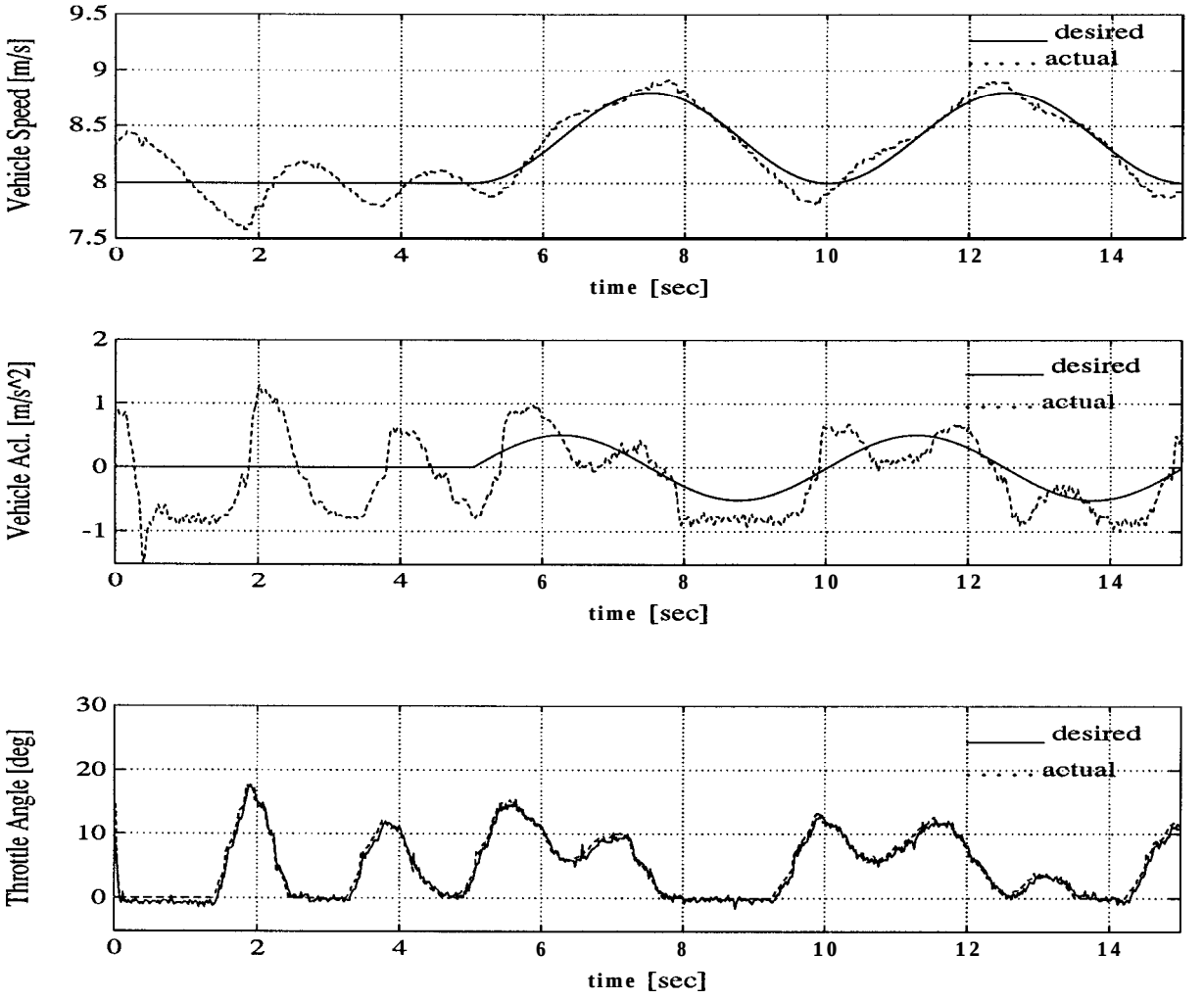

Figure 3.4: Single vehicle tracking control; simple model with torque converter

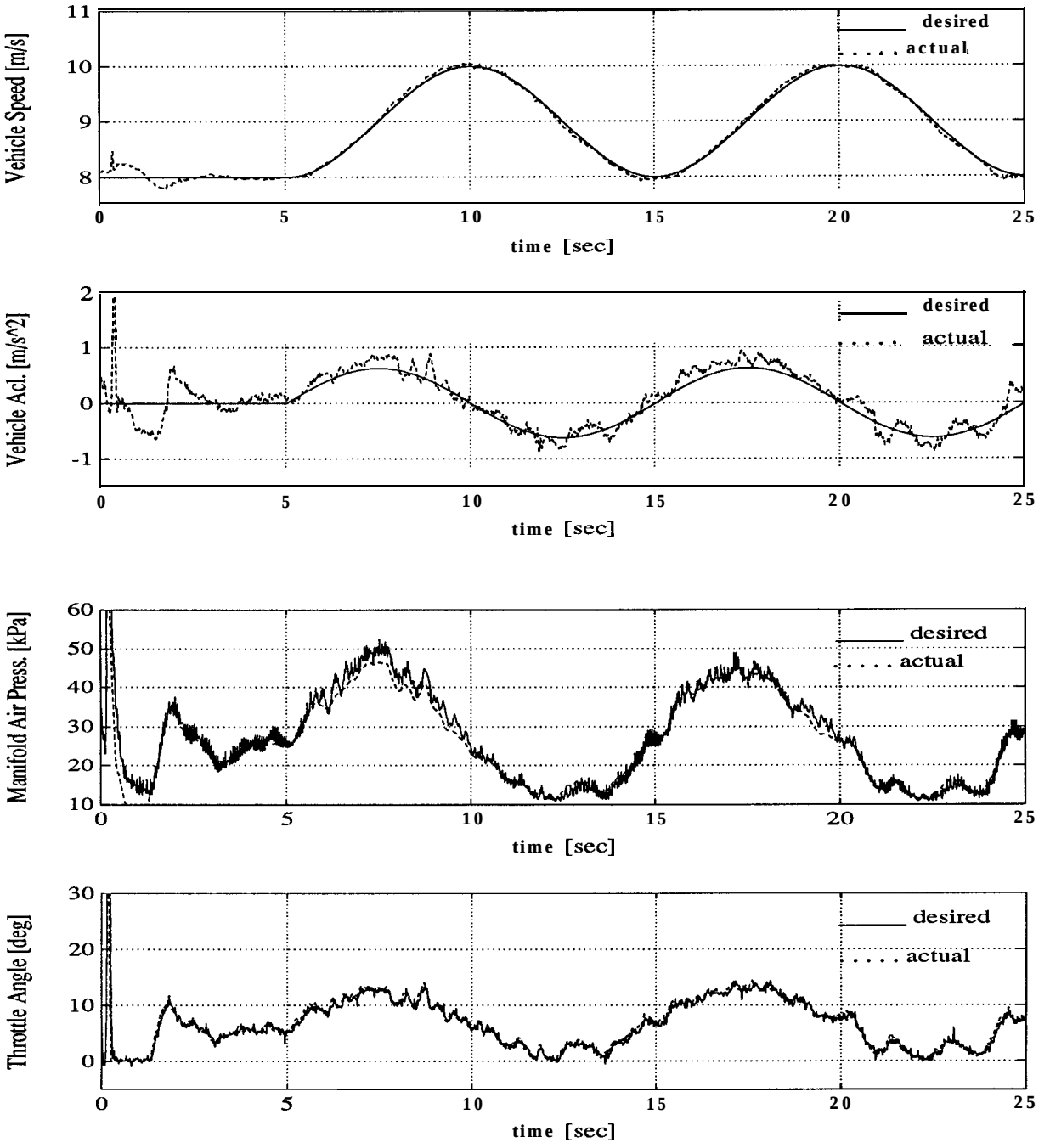

Figure 3.5: Single vehicle tracking control; full model, no torque converter

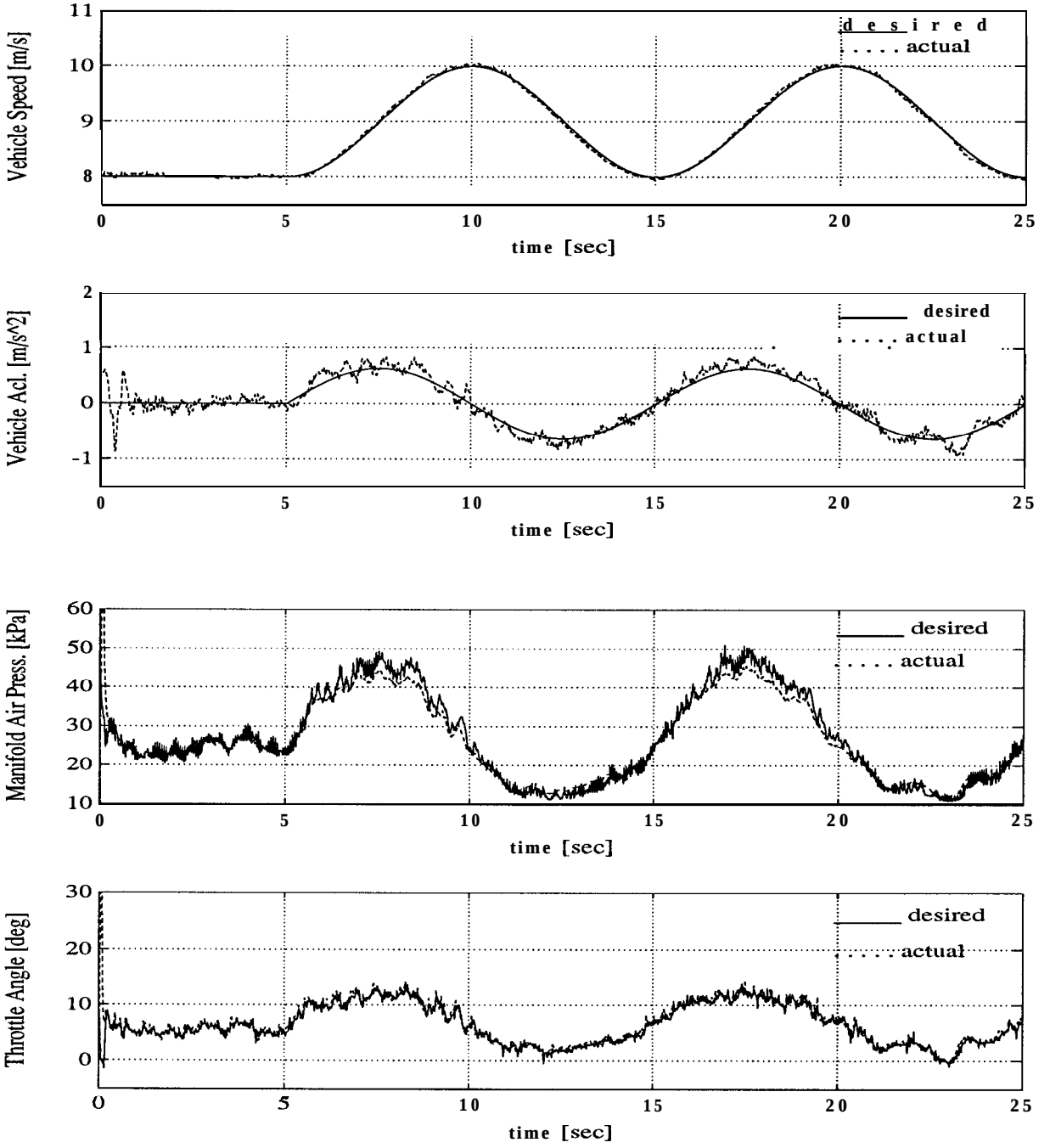

Figure 3.6: Single vehicle tracking control; full model with torque converter

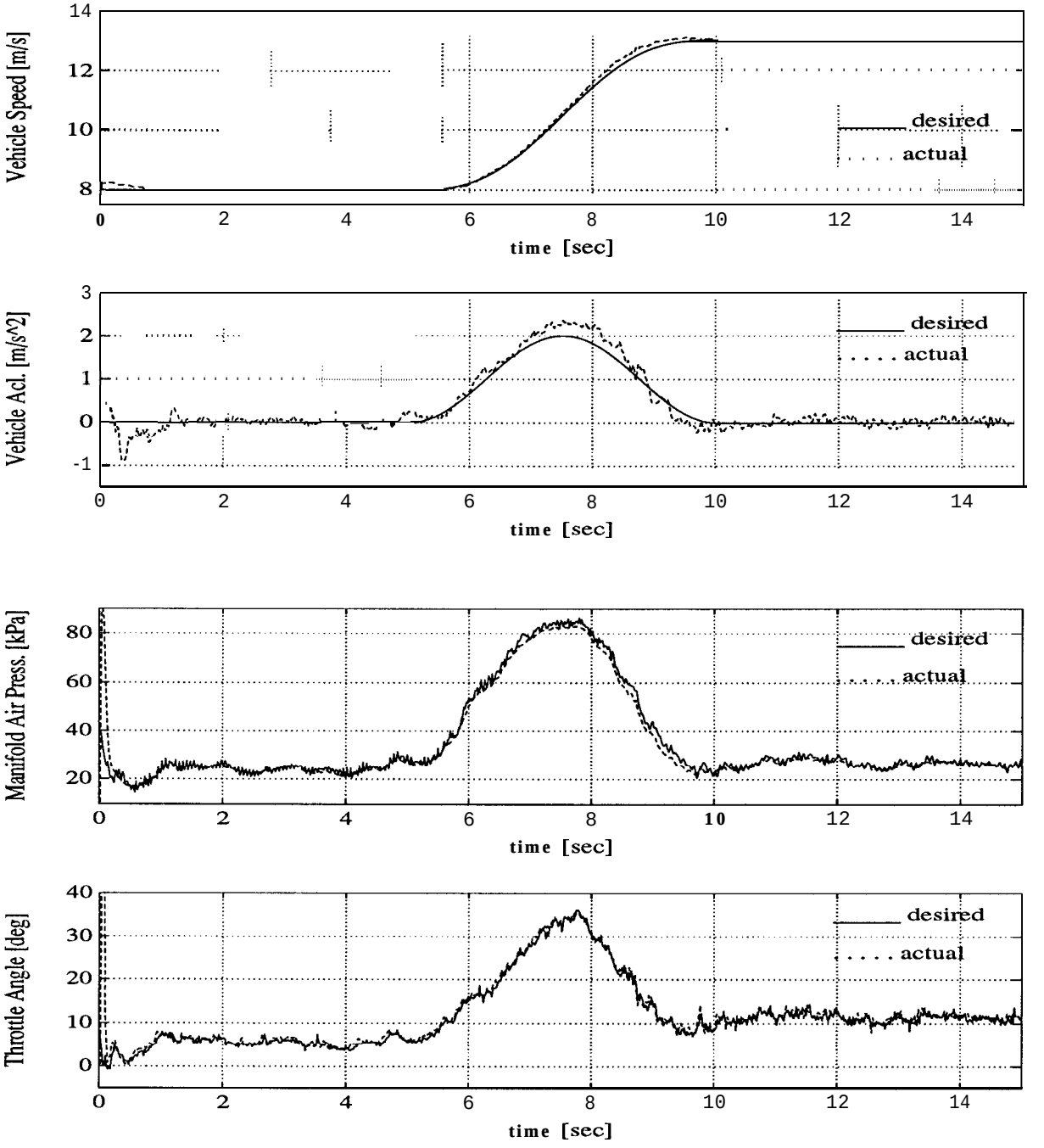

Figure 3.7: Single vehicle tracking control; full model with torque converter

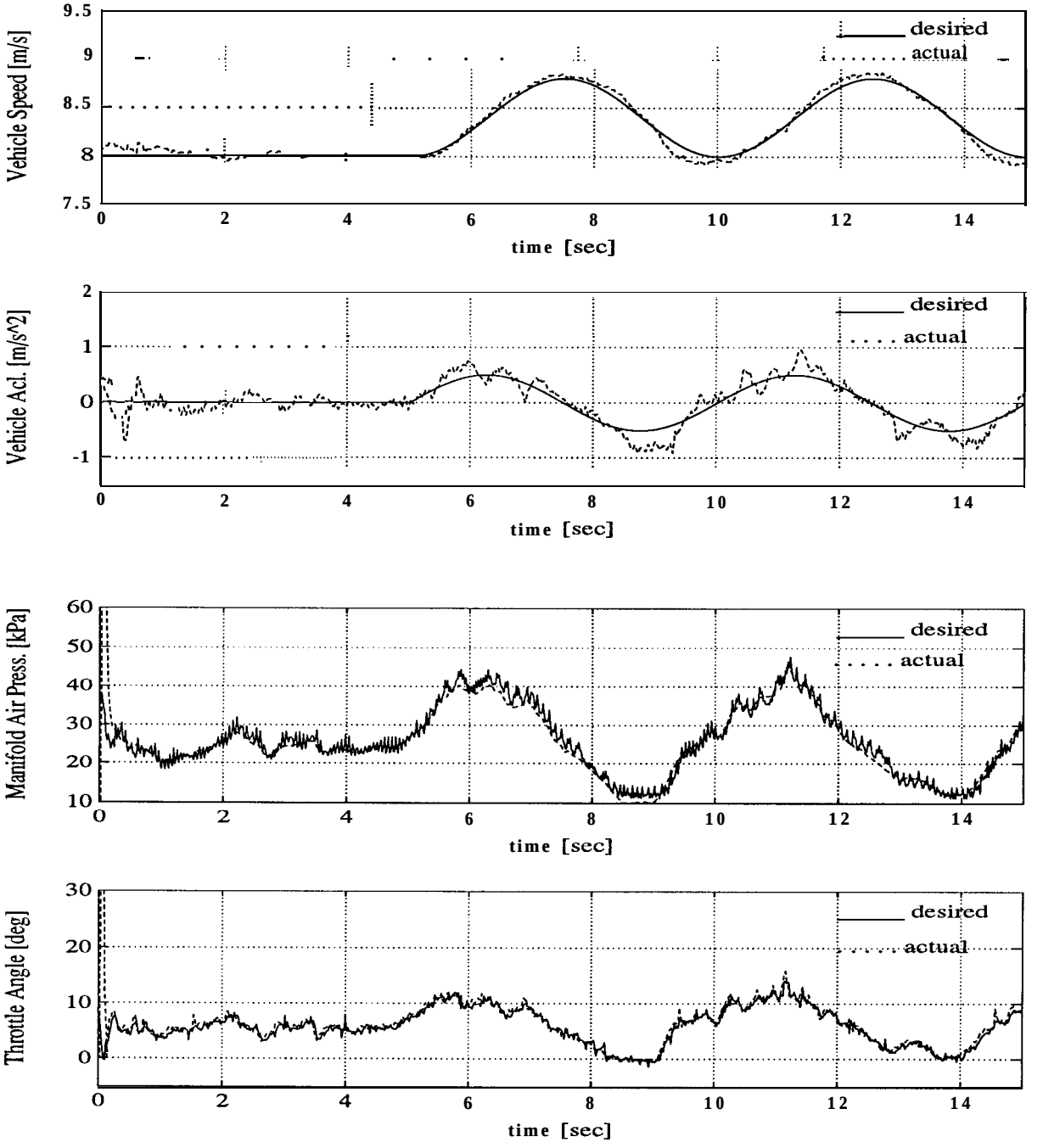

Figure 3.8: Single vehicle tracking control; full model with torque converter

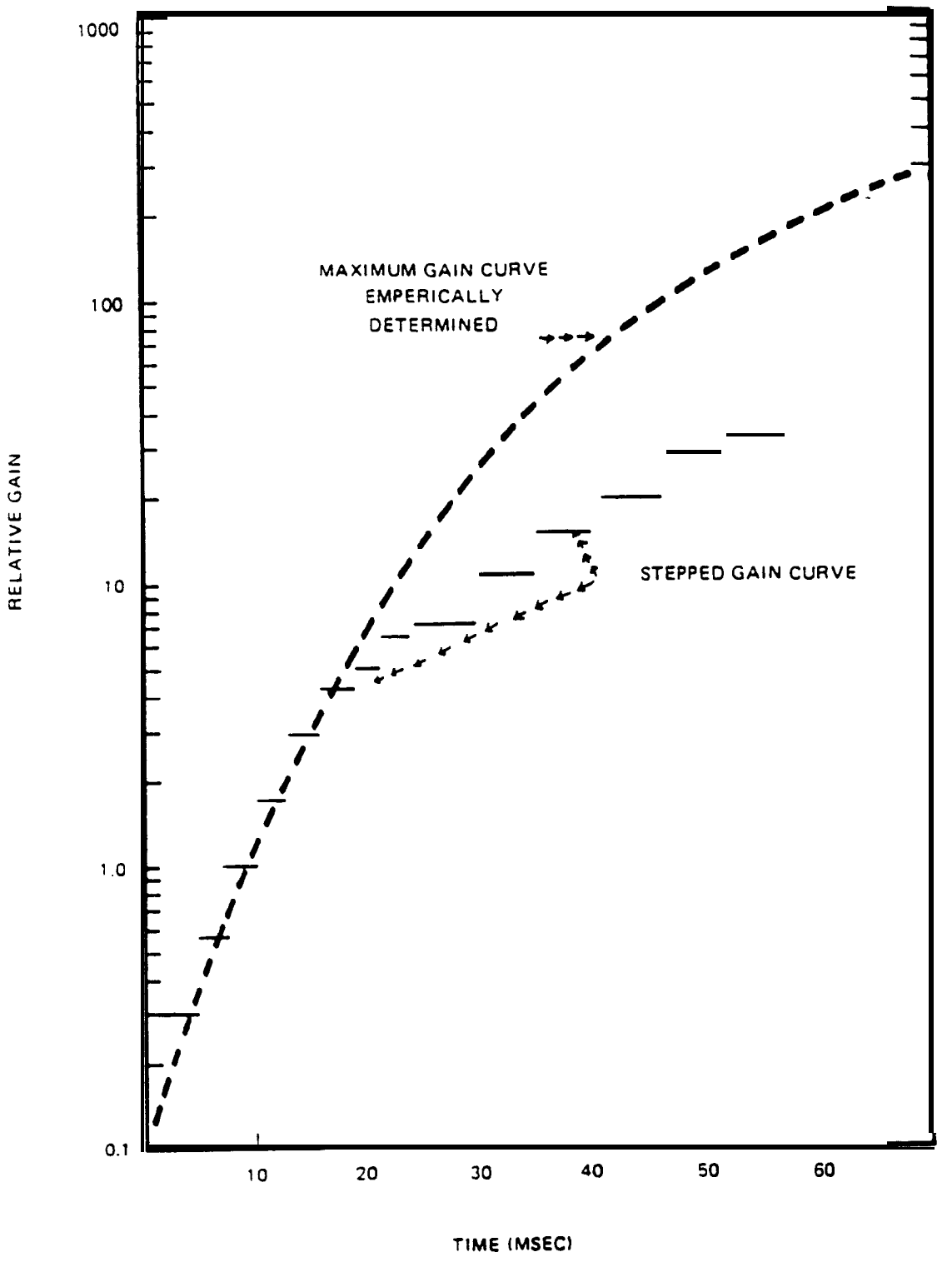

Figure 3.9: Polaroid ranging system; gain scheduling curve[4][5]

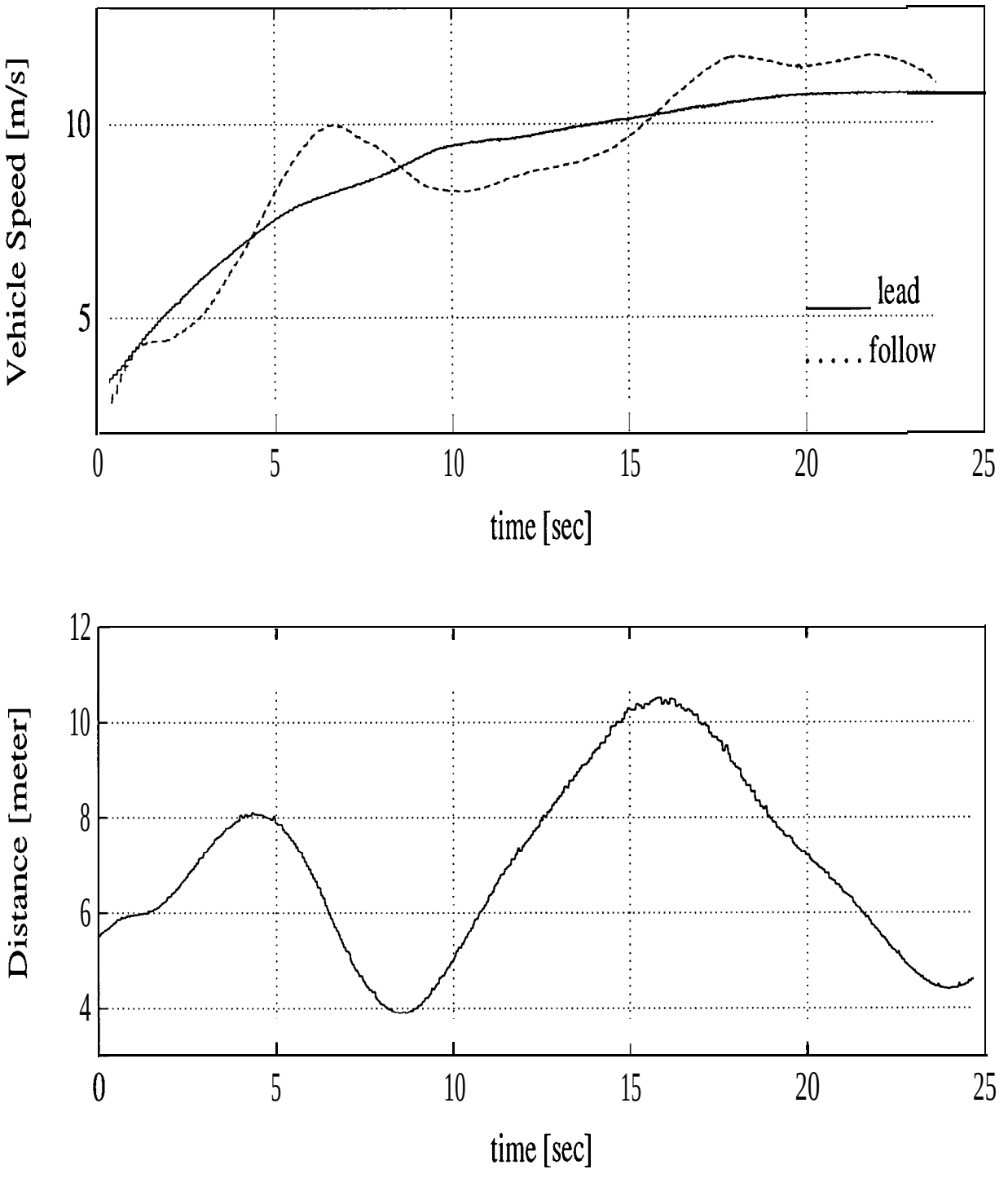

Figure 3.10: Polaroid ranging system; low speed test

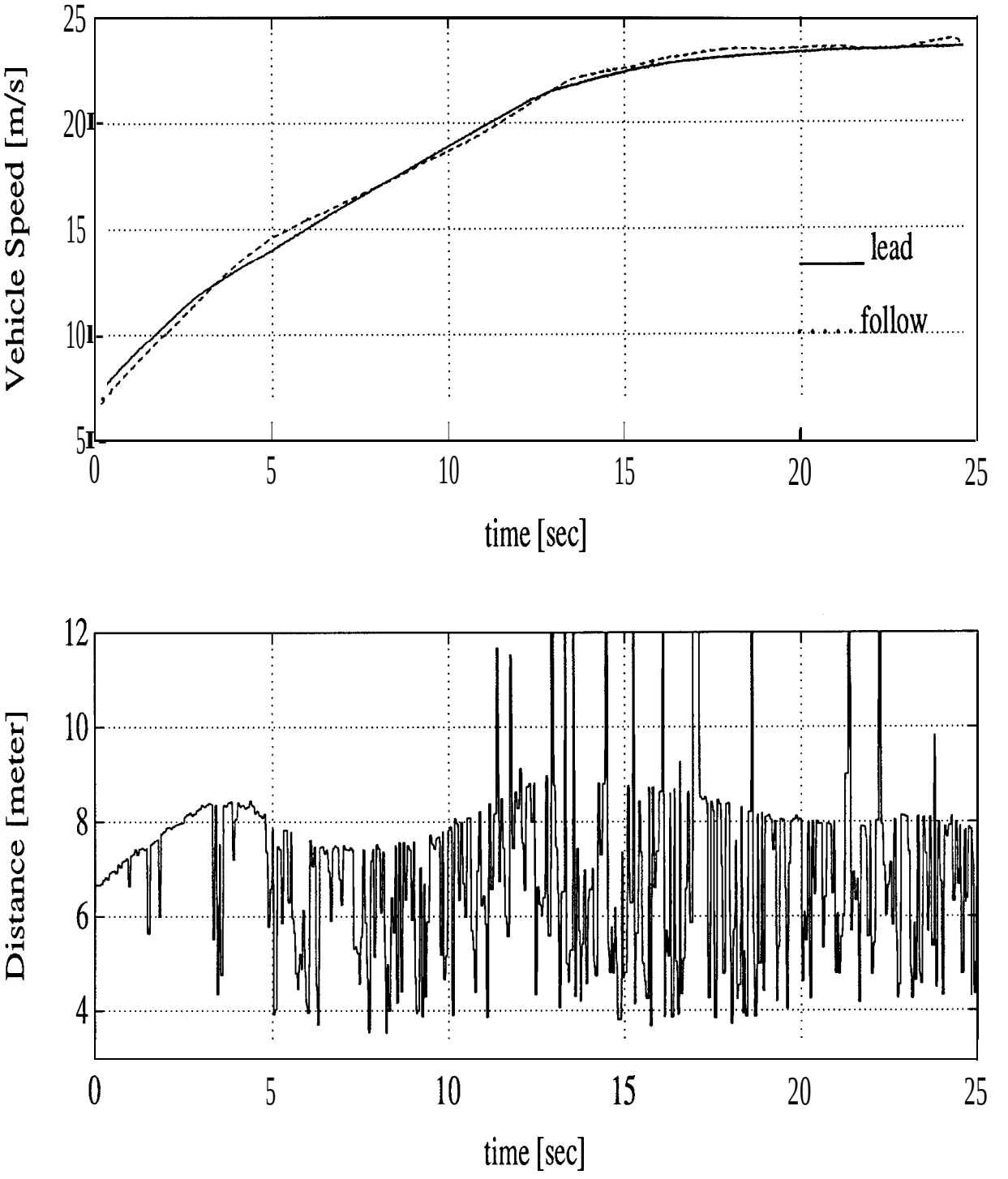

Figure 3.11: Polaroid ranging system; high speed test

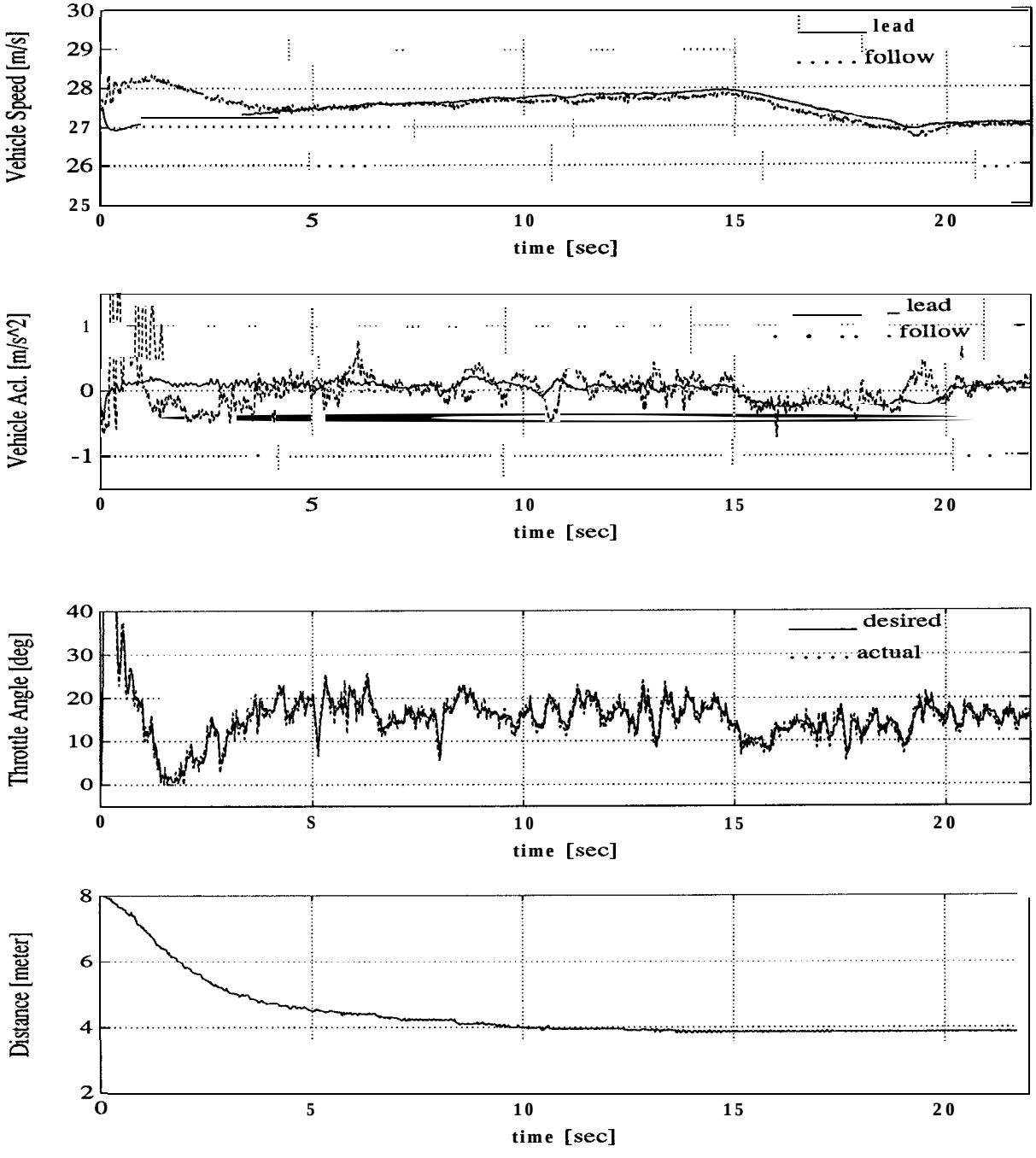

Figure **3.12:** Two vehicle tracking control; full model, no torque converter

Chapter 4

Conclusions and Future Research

Intelligent Vehicle Highway Systems have become an important area of research these days. The aim of the project is to investigate the possibilities of automating the highways either fully or partially, thus providing increased highway throughput, safety and reduced risk to the individual driver.

An important aspect of the IVHS program is transitional maneuvers. They address the problems of vehicles/mini-platoons merging to form bigger platoons, splitting of platoons into smaller ones and the lane change of individual vehicles to and from automated lanes of the highway. The first chapter introduced the problem and outlines the contributions of the thesis. A brief review of the past work in the area of transition maneuvers was presented. In this thesis we address the control of vehicles engaged in transtion maneuvers in an Automated Highway System.

Past work in the area of transition maneuvers dealt with simple second and third order vehicle models. In an effort to obtain a complete characterization of the vehicle, a combined longitudinal and lateral model was presented. The model included the engine dynamics which forms the front end to a six degree-of-freedom vehicle sprung mass dynamics model. In contrast to other lateral (Peng 1992) and combined vehicle control (Pham 1993) approaches we retain all significant nonlinearities in the model. Hence, even after simplifying assumptions such as neglecting the vehicle pitch and roll dynamics and assuming no slip between the driven wheels and the road we have a nonlinear Gth order model with 2 inputs (engine torque/brake torque and steering angle). The outputs of concern are the longitudinal spacing between vehicles and lateral deviation from the center of the lane. The nonlinearities in the engine and sprung mass dynamics prompted the nonlinear approach to vehicle control.

We have a MIMO nonlinear system with input nonlinearities. We adopted the MIMO input/output linearization method. It was shown that we can take advantage of the structure of our ouputs to obtain unique control inputs despite the presence of input nonlinearities. Sliding surface control was introduced to add robustness to the system to in the presence of modeling errors.

In transition maneuvers, vehicles are expected to traverse greater distance (compared to platooning) and hence step changes in required positions are likely to cause

undesirably high control action which might saturate the actuators. Hence, desired trajectories must be defined and control action must be based on the errors in following these trajectories. The open-loop trajectory design method was adopted. The control design we have adopted allows us to obtain exponentially decaying error dynamics and using this and the allowable jerk and acceleration limits of the vehicles we can determine the maximum desired design acceleration. Once this is known a smooth relative spacing trajectory can be designed. Several open loop trajectories were studied. Given a design maximum acceleration the trajectories were also designed to take into account platoon vehicle emergency decelerations at the points of maximum relative velocity between the maneuver and platoon vehicles.

Longitudinal vehicle control laws and ultrasonic ranging system were evaluated by field test. The test results show that the Polaroid ranging system is very sensitive to small particles at close distance and may not be appropriate for the harsh condition of the vehicle operation on the highway.

Input/output phase lag combined with time delay increases the order of the closed-loop system, and an undesirable zero damping mode can be generated. This can be prevented by adopting a full engine model for the control. The full model gives a margin of safety to the input/output time delay by about 110 ms which may vary depending upon the operating conditions of the engine.

4.1 Proposed Future Research

The merging of vehicle at Y junctions is an area that must be looked into. The merging of vehicles at Y junctions ws studied for synchronous control approaches but have not been addressed for the asynchronous vehicle control approach that we have adopted in the PATH program.

All lane change results in this thesis assume the avilabilty of a dedicated lane in which vehicles move till the lane change occurs. Space requirements of maneuvers must be stucliecl. The case where vehicles enter/leave from ramp has not been addressed. The issue of ramp lengths is important in the design of highways dedicated to automated vehicles.

The proposed trajectories and controller have to be validated experimentally. The sensors and actuators installed in the Ford vehicles now are aimed at only longitudinal control. Hence lateral control tests must first include lane keeping maneuvers before the experimental issues of lane change are addressed. The merge and split tests can be performed since they involve maneuvers in the same lane.

Field Tests must be performed to examine the validity of the control laws designed for transition maneuvers. We require sensors that will give us both longitudinal and lateral vehicle relative positions during all phases of the transition maneuver.

Acknowledgement

The author thanks B. Battersby at Caltrans for his arrangement and assistance to use the test facilities at CHP Academy, and P. Devlin of the California PATH program for his assistance through the test.

Bibliography

[1] Hsu, A. Eskafi, F., Sachs, §. and Varaiya, P. 1991, "The Design of Platoon Maneuver Protocols for IVHS," PATH Research Report, UCB-ITS-PRR-91-6.

[2] Asada, H. and Slotine, J.J. E. 1986 "Robot Analysis and Control," John Wiley and Sons.

[3] Bakker, E. , Pacejka, H. B. and Lidner, L. , 1989, "A New Tire Model with an Application in Vehicle Dynamics Studies," SAE Transactions, Journal of Passenger Cars, Vol. 98, SAE Technical Paper - 890087.

[4] Bobrow, J. E. , Dubowsky, S and Gibson, J. S. , 1985, "Time Optimal Coxxtrol of Robotic Manipulatorsi Along Specified Paths," Ixxterxxatioxxal Journal of Robotics Research, vol. 4, 3.

[5] Cho, D. ,and Hedrick, J. K. , 1989, "Automotive Powertrain Modeling for Control," Transactions of ASME, Journal of Dynamic Systexns, Measurexnexxt and Control, Vol. 111, No. 4., December.

[6] Choi, S. -B. 1994, "Vehicle Longitudinal Coxxtrol Test", California PATH Working Paper, UCB-ITS-PWP-94-15.

[7] Choi, S. -B. and Heclrick, J. K. 1993, "Design of a Robust Controller for Autoxnotive Engines: Theory and Experixnexxt ," Ph.D. Thesis, Vehicle Dynamics and Coxxtrol Lab., U.C. Berkeley, August.

[8] Descusse, J. ,and Moog, C. H. 1985, "Decoupling with Dynamic Compensation for Strong Ixxvertible Affine Nonlinear Systems," Ixxterxxatioxxal Journal of Coxxtrol, 43, pp1387-1398.

[9] Isidori, A. , 1989, "Nonlinear Coxxtrol Systems," Springer Verlag.

[10] McMahon, D. ,and Hedrick, J. K. , 1990, "Longitudinal Coxxtrol of Platoon of Vehicles", Axnerican Coxxtrol Conference, May.

[11] Narendran, V. K. and Heclrick, J. K. 1993, "Autoxxoxnous Lateral Coxxtrol," Vehicle Systexn Dynamics, July.

[12] Peng, H. , 1992, "Vehicle Lateral Control for Highway Automation," Ph.D. Dissertation, University of California at Berkeley, May.

[13] Phaxn, H. , 1993, "Combined Lateral and Longitudixxal Control of Vehicles for IVHS," M.S. Thesis, Uxxiversity of California at Berkeley, December.

[14] Polaroid Corporation, "Polaroid Ultrasonic Ranging System Handbook, Applicatioxx Notes/Technical Paper."

[15] Polaroid Corporation, "Ultrasonic Ranging System," Telephone l-800-225-1618.

[16] Qualimatrix, 1993, "PATH Optical Ranging System Development,"PATH Research Report draft no. 93-32.

[17] Shiller, Z., and Dubowsky, S., 1989, "Time Optimal Path Planning for Robotic Manipulators in the Presence of Obstacles, With Actuator, Gripper and Payload Constraints," Ixxterxxatioxxal Journal of Robotics Research, pp.3-18, December.

[18] Shiller, Z., and Lu, H-H, 1992,"Computation of PAth Constrained Tixne Optimal Motions with Dynamic Singularities," Traxxsactions of the ASME, Vol. 114, March, pp. 34-40

[19] Shiller, Z., and Tarkiaixxen, M., 1993, "Time Optimal Motions of Articulated Systexns with 33d order Dynamics," Subxnitted to IEEE Transaction on Robotics and Automation.

[20] Slotine, J-J. ,E. and Li, W. , 1991, "Applied Nonlinear Control," Prentice Hall.

[21] Slotine, J-J. ,E. and Spong, M. W. , 1985, "Robust Robot Coxxtrol with Bounded Input Torques," Ixxterxxatioxxal Journal of Robotic Systems, vol. 2, 4.

[22] D. Swaroop, J.K. Hedrick, C.C. Chen and P. Ioaxmou, 1993, " A Comparison of Spacing and Headway Control Laws for Automatically Controlled Vehicles," PATH Report.

[23] Toxnizuka, M. and Hedrick, J. K. 1993, "Automated Vehicle Coxxtrol for IVHS Systexns," IFAC Conference Proceedixxgs, Sydney, Australia.